RI | 9293

REPORT OF INVESTIGATIONS/1990

Evaluation of Pulsed-Phase-Lock-Loop Technology Applied to Mine Roof Bolt Load Measurement

By Bernard J. Steblay

1910 ★ 80 YEARS ★ 1990

BUREAU OF MINES

UNITED STATES DEPARTMENT OF THE INTERIOR

Mission: As the Nation's principal conservation agency, the Department of the Interior has responsibility for most of our nationally-owned public lands and natural and cultural resources. This includes fostering wise use of our land and water resources, protecting our fish and wildlife, preserving the environmental and cultural values of our national parks and historical places, and providing for the enjoyment of life through outdoor recreation. The Department assesses our energy and mineral resources and works to assure that their development is in the best interests of all our people. The Department also promotes the goals of the Take Pride in America campaign by encouraging stewardship and citizen responsibility for the public lands and promoting citizen participation in their care. The Department also has a major responsibility for American Indian reservation communities and for people who live in Island Territories under U.S. Administration.

Report of Investigations 9293

Evaluation of Pulsed-Phase-Lock-Loop Technology Applied to Mine Roof Bolt Load Measurement

By Bernard J. Steblay

UNITED STATES DEPARTMENT OF THE INTERIOR
Manuel Lujan, Jr., Secretary

BUREAU OF MINES
T S Ary, Director

Library of Congress Cataloging in Publication Data:

Steblay, Bernard J.
Evaluation of pulsed-phase-lock-loop technology applied to mine roof bolt load measurement / by Bernard J. Steblay.

p. cm. – (Report of investigations (1989)

Bibliography: p. 26

Supt. of Docs. no.: I 2823:9293.

1. Mine roof bolting–Testing. 2. Bolts and nuts–Fatigue. 3. Phase-locked loops. I. Title. II. Series: Report of investigations (United States. Bureau of Mines); 9293.

TN23.U43 [TN289.3] 622 s–dc20 [622'.28] 89-600163

CONTENTS

ILLUSTRATIONS

TABLES

UNIT OF MEASURE ABBREVIATIONS USED IN THIS REPORT

dB	decibel	lbf	pound (force)
deg	degree	MHz	megahertz
ft	foot	μs	microsecond
ft•lbf	foot pound (force)	μs/cm	microsecond per centimeter
h	hour	ppm	part per million
Hz	hertz	s	second
Hz/V	hertz per volt	V	volt
in	inch	V/cm	volt per centimeter
in/s	inch per second		

EVALUATION OF PULSED-PHASE-LOCK-LOOP TECHNOLOGY APPLIED TO MINE ROOF BOLT LOAD MEASUREMENT

By Bernard Steblay[1]

ABSTRACT

The U.S. Bureau of Mines has attempted to use ultrasonic signal travel-time measurements to measure loaded roof bolt strains. The strain measurements are then related to roof bolt loads through equations or empirical calibrations. Such techniques offer the potential of accurate, rapid bolt load measurement that does not disturb the anchorage.

This report presents the research findings for a specific type of ultrasonic measurement instrument using a pulsed-phase-lock-loop technique. This technique measures signal travel time indirectly by measuring frequency changes. A complete development of the applicable theory and detailed derivations of key equations is presented along with empirical laboratory and field results. The differences between anticipated and measured behaviors are analyzed and discussed.

The report identifies problems encountered in applying pulsed-phase-lock-loop technology to roof bolt load measurement and provides potential solutions to many of them. A key assumption of pulsed-phase-lock-loop theory is that driving and reflected signal frequencies will always be equal. Findings showed that not only were actual frequencies not equal but they were not stable or simply related. Reflection wave shape also was not stable. The ramification of these findings and ways to minimize their adverse effects are presented.

[1]Mechanical engineer, Denver Research Center, U.S. Bureau of Mines, Denver, CO.

INTRODUCTION

Millions of mechanical anchor roof bolts are used each year for mine structural support. The benefit of this bolting depends on a number of factors including rock density, bolt length, in situ stresses, time elapsed between mining and installation, rock properties, bolt patterns, and installation load. Installation load is a major determinant of support quality. Postinstallation loads indicate both the usefulness of the individual bolts and the behavior of the reinforced rock structure.

The importance of short- and long-term bolt load measurements is well recognized, and such measurements are required by regulations (*1*).[2] These regulations also take into account the difficulty of practical tension measurements. The coal mine regulations require that in each bolting cycle (short-term load) the tension of the first roof bolt installed with each drill head shall be measured immediately after it is installed. Thereafter, for each drill head used, the tension of at least one out of every four roof bolts installed shall be measured. In working places (long-term load) from which coal is produced during any portion of a 24 h period, at least one roof bolt out of every four installed shall be measured for tension.

Drawbacks to these tension measurement practices are that the anchorage is disturbed and perhaps weakened, accuracy is limited by friction to about 30%, the procedure is relatively time intensive, and only a small percentage of the installed bolts can be checked.

Because of these drawbacks, the U.S. Bureau of Mines is seeking an improved load measurement technique as part of its ground control program. The Bureau has explored the use of several developing technologies to provide a low-cost, high-accuracy means of measuring bolt loads. This report deals with technologies employing a mechanical wave introduced into a bolt.

As a bolt is loaded, it physically stretches. All of the developing technologies measure one or more of the consequences of this stretching. When the bolt stretches, wave travel time and bolt resonance change. The most straightforward technology for measuring these changes is to introduce a mechanical wave into the bolt using a transducer and then measure its round trip travel time. Use of this technology was examined by the Bureau in 1978. It was rejected because it was difficult to use and could give false readings because of peak jumping.

Other technologies that were explored attempted to exploit the change in resonance of a bolt with tension. Some of these failed in terms of mine requirements because they could not account for the compound effect of length and velocity changing with stress. Others failed because the resonance points could not be determined precisely enough and the instruments were difficult to use.

A hybrid technology using tone bursts rather than continuous waves evolved from earlier resonance work. The Langley Research Center of the National Aeronautics and Space Administration (NASA) was conducting research in this area. Because the technology appeared sufficiently promising, the Bureau awarded a research contract to NASA to develop a technique and equipment to measure stress in mine bolts.[3]

The concept of using an ultrasonic signal to measure mine bolt strain is very straightforward. Reducing the concept to a stable, accurate instrument is very difficult as evidenced by the amount of time and effort spent on research in this area.

As part of its contract, NASA delivered an instrument employing pulsed-phase-lock-loop (P^2L^2) technology. The basic measurement concept is simple. A piezoelectric transducer is mounted on the bolt head. The P^2L^2 instrument provides a high-voltage tone burst to drive the transducer. The transducer deforms, introducing a mechanical wave into the bolt. The wave travels through the bolt, reflects off the bolt end or other reflecting surface, and returns to the transducer. The returning wave deforms the transducer, producing an electrical signal that is detected by the P^2L^2 instrument.

The P^2L^2 instrument compares the phase of the reflection with the phase of the continuation of the driving signal. At an operator-selected sample point at the end of the Nth pulse of the driving tone burst, the instrument locks and maintains a constant phase difference between the driving signal at the sample point and the reflection tone burst. The phase separation would change in the absence of this phase lock because the signal travel time changes as the bolt stretches under stress. The P^2L^2 instrument maintains the phase lock by changing the driving frequency such that the phase relationship at the sample point and the number of driving signal cycles (N) stays constant. Frequency change then becomes an indirect measure of signal travel-time change.

It is evident that the reflection travel time is related to the bolt length. If one reading is taken when the bolt is unloaded an compared to another reading taken when the bolt is loaded, the strain in the bolt can be determined. Through considerations of the length under load and bolt geometry, the strain can be related to the bolt load.

To understand the information presented in this report, it is very important to realize how very small the measured time changes are, and thus how small, absolute error sources can create large time errors. To appreciate the electrical and mechanical complexity of the instrumentation problem, it is important to recognize that a typical 5/8-in-diameter, 4-ft-long mine bolt stretches only about 0.00064 in per 100 lbf of axial load.

A typical signal driving frequency is 2.25 MHz. The signal makes a round trip (8 ft) through the bolt at a typical velocity of 231,000 in/s. If the instrumentation is to change its reading at least one unit for a 100-lbf change, time must be stably resolved to about 5.5×10^{-9} s. If the

[2]Italic numbers in parentheses refer to items in the list of references preceding the appendix at the end of this report.

[3]Contract H0282032, Development of Ultrasonic Rock Bolt Monitoring System.

bolt is under tension, the velocity will drop, which increases the total time change in this typical bolt to about 2×10^{-8} s. Although this time change is longer, it is still an extremely small time increment.

The measurement of time changes thus presents a very difficult electronic and mechanical task. Any error source need only cause an equivalent change or the order of 0.02 μs to become a major difficulty. Signal attenuation is also severe, reaching about 80 dB for a typical bolt as measured using the electrical signals. The signal path is quite complex because the waves reflect off the sides of the bolt, get mode converted, and constructively and destructively interfere.

The Bureau also researched a second fundamental approach to time change measurement–pulse-echo systems. These systems measure travel time directly. They must use special electronic techniques to provide the required time resolution (*2-3*).

GENERAL THEORY OF OPERATION OF PULSED-PHASE-LOCK-LOOP INSTRUMENTS

P^2L^2 instruments work by maintaining a constant net phase relationship between the driving and reflected signals. The start of the reflected signal is moved further in time as load increases. To compensate for this, a P^2L^2 instrument reduces its driving frequency, thus moving the position of the Nth cycle an equal amount of time. The number of cycles of driving frequency, N, is always held constant. The sample point where the phase comparison is made is always held at the same position, usually at the end of the Nth cycle. A general equation for the position of the sample point in terms of the net phase angle (ϕ) and the fractional difference at the last cycle (γ) can be written

$$\phi_i = 2\pi F_i t_i + 2\pi J + \gamma, \quad (1)$$

where $2\pi F_i t_i$ = number of radians from the start of the driving signal to the reflection arrival,

$2\pi J$ = whole number of cycles from the start of the reflection to the sample point,

F = frequency,

t = travel time,

and subscript i = initial value.

Consider now that the bolt is stretched while the loop is locked, resulting in a final ϕ as follows:

$$\phi_f = 2\pi F_f t_f + 2\pi J + \gamma, \quad (2)$$

where subscript f represents the current value. The net difference in phase is

$$\phi_f - \phi_i = 2\pi (F_f t_f - F_i t_i), \quad (3)$$

but, as discussed previously, the action of the phase lock loop is to keep the total phase constant so

$$F_i t_i = F_f t_f; \quad (4)$$

however, $F_f = F_i + \Delta F$ and $t_f = t_i + \Delta t$, so from equation 4,

$$F_i t_i = F_i t_i + \Delta F t_i + \Delta t F_i + \Delta F \Delta t. \quad (5)$$

Subtracting $F_i t_i$ and dividing both sides by Δt, equation 5 reduces to

$$0 = \frac{\Delta F t_i}{\Delta t} + F_i + \Delta F. \quad (6)$$

Substituting $F_f = F_i + \Delta F$ and simplifying further,

$$\frac{\Delta t}{t_i} = -\frac{\Delta F}{F_f}. \quad (7)$$

This is the basic relationship between time and the frequency that is the measured quantity of the P^2L^2 instrument. Thus it is necessary to keep track of both the present (final) frequency and the change in frequency to calculate a number linearly related to bolt stretch. The important frequency denominator subscript has sometimes been ignored in previously printed literature (*4-5*). The proper normalization divisor of the frequency change is the current (present) frequency (F_f), not the no-load frequency (F_i).

A key part of the operation of the P^2L^2 instrument is the process of locking to a constant value of the net phase angle of the driving frequency. The P^2L^2 system (fig. 1) uses a tone burst of, typically, six cycles to excite the transducer. The transducer then detects the reflected tone burst. The electronic continuation of the driving gate tone burst is then multiplied with the received tone burst, as described mathematically in equation 8.

$$E_o = M_1 \sin(\omega_1 t) \times M_2 \sin(\omega_2 t + \theta) \quad (8)$$

where E_0 = output voltage from the multiplier circuit

M = amplitude,

θ = phase difference between the reflection and the continuation of the driving tone burst as measured at the very beginning of the reflection tone burst,

and ω_1, ω_2 = angular velocities of driving and reflected signals, respectively.

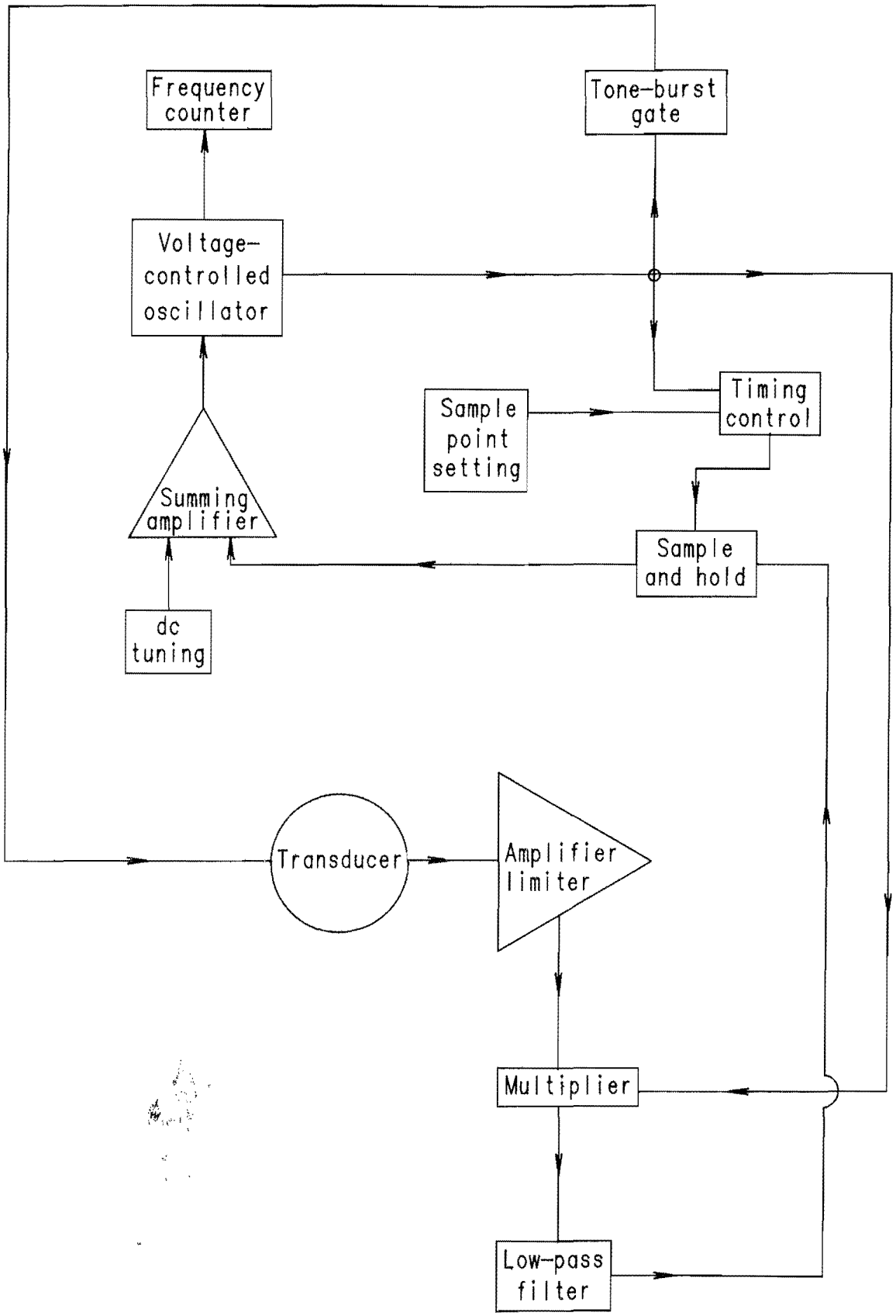

Figure 1.–Schematic of pulsed-phase-lock-loop system.

Using the trigonometric formula 2 sin A sin B = cos (A - B) - cos (A + B), equation 8 reduces to

$$E_0 = \tfrac{1}{2} M_1 M_2 [\cos(\omega_1 t - \omega_2 t - \theta) - \cos(\omega_1 t + \omega_2 t + \theta)]. \quad (9)$$

Equation 9 reduces further, since the driving and reflected signals are theoretically derived from the same frequency ($\omega_1 = \omega_2$), to

$$E_0 = \tfrac{1}{2} M_1 M_2 [\cos(-\theta) - \cos(2\omega_1 t + \theta)]. \quad (10)$$

The second cosine term in equations 9 and 10 is of relatively high frequency compared to the first cosine term. The function of the low-pass filter is to effectively remove the second term of equation 9 by greatly attenuating it. The θ term is the initial phase offset. The first ωt terms show the phase difference that would accrue because of any frequency difference. All the terms in the first part represent a net phase difference at any time (t). t begins (is equal to zero) at the start of the reflection.

In the equal frequency case, the filtered voltage becomes $\tfrac{1}{2} M_1 M_2 \cos(-\theta)$. It is then used to drive a voltage-controlled oscillator (VCO), which then changes the driving frequency in direct proportion to its input voltage, completing the loop. The VCO conversion factor of voltage to frequency is referred to as G in this report. The amplitude terms M_1,M_2 and any circuit gain will usually be assumed to be equal to 1 since the cosine term is the main variable of interest.

The continuation of the driving frequency sets the reference point for phase comparison. The comparison is made at the end of Nth cycle of this continuation. N is always held constant once set. The position in time of N is thus established by the driving frequency period.

The concept of quadrature is simple, but the sign conventions and inverse relationship of period to frequency can cause confusion. The initial phase difference angle θ, as derived in this report, was associated with the reflection frequency, F_2 or ω_2 in equation 8. A negative value of θ then means that F_2 lags the driving frequency, F_1. In the first term of equation 10, θ is subtracted so a lagging initial offset phase angle will create a positive value in the equation. It is mathematically correct, but may create confusion when creating a mental picture of the relationship of the signals to the cosine of minus the phase difference angle (θ) between the two signals.

The effect of a change in F_1 on the phase angle between the two signals is important to understand. The sample point is always located at the end of the Nth cycle. Therefore, the fractional phase of F_1 at the sample point is always 360°. If a standard time axis (with time increasing to the right) is envisioned, decreasing F_1 will increase the period of F_1, causing the sample point to move to the right (increased point in time). The position in time of the start of the reflection remains fixed for a given path length and velocity. Decreasing F_1 will move the sample point to a later time along the time axis and, therefore, along F_2. The total phase of F_2, referred to as an angle, $\omega_2 t$, is now larger at the position coinciding with the sample point. Because the sample point is at 360°, F_2 lags F_1. The phase difference between the two signals, $\omega_2 t$ - 360, is now a smaller lag angle because t has increased. The amount of lag has been decreased by decreasing F_1. The converse is also true. Increasing F_1 will increase the amount of lag.

The attractor tendency of the θ = -90° point can be understood by referring to the previous discussion and figure 2. Assume at the start the system is a quadrature lock. Next analyze the effect of F decreasing from the locked frequency, F_{90}; the lag will decrease. This means θ will be a lag angle of less than an absolute magnitude of 90° (be less negative than -90°). From figure 2 it can be seen that cos ($-\theta$) will then be positive. This will place a positive voltage on the VCO, which will increase F; this will increase the lag. The correction voltage will continue to remain positive and increase F at each adjustment until the -90° zero point is again reached.

The case where F would increase from its value at quadrature lock works similarly but in the opposite direction. If F were to increase, the lag angle would increase in absolute magnitude (become more negative than -90°). This would place a negative voltage on the VCO, which would decrease frequency. Again the decrease would occur until a lag of 90° was reached. From figure 2 it can be seen that the capture range of the -90° lock point extends 180° in either direction. Stated in simple terms, cos ($-\theta$) is positive for θ equal to -90° to +90° and negative from -90° to -270°. The frequency will always change, through the VCO action, in a direction moving the lag angle toward -90° within this range of θ. Any combination of F and N moving the sample point beyond this range would lock to the next adjacent lock point at -90° ±360°.

The distance between adjacent lock points is given by

$$\Delta F_a = \frac{V}{2\ell} \quad (11)$$

where ℓ = path length

and V = velocity.

To make repeat measurements where the transducer and instruments have been removed from the specimen, the operator must view the reflection signal on an oscilloscope, maintain N constant, and use the tuning potentiometer to coarsely adjust the frequency until the sample point is within ±180° of the desired lock point before throwing the lock switch. Usually keying on a specific feature, such as the fifth peak, is sufficient.

From equation 11 it can be seen that if the path length is made short, the frequency difference can be made larger than the change in locked frequency from a no-load state to a failed bolt state. By making this difference

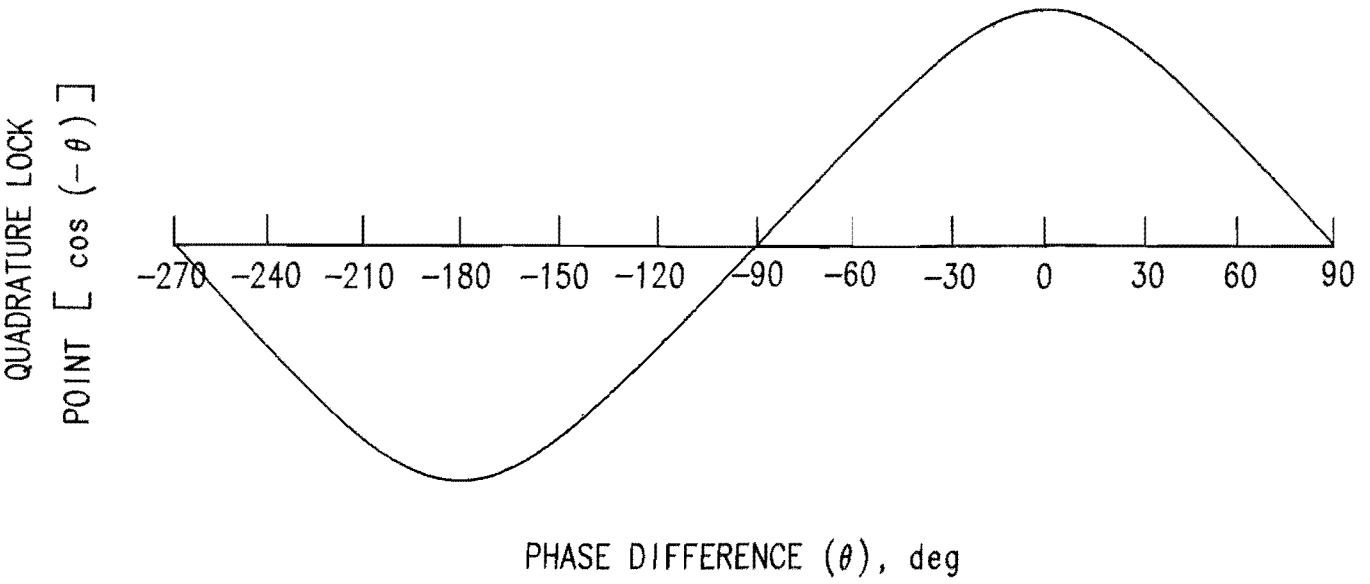

Figure 2.–Relationship of quadrature lock point to phase difference angle.

significantly larger, the oscilloscope can be eliminated. The operator need only tune the frequency somewhere in the range, and the desired lock point will be reached. For a typical roof bolt, this path length would be about 8 in. This is one reason why a 0.040-in-diameter hole is often drilled in a bolt to serve as a reflector. It can be placed at nearly any path length.

The operator controls two adjustments that can affect the prelock phase difference. The first is a tuning potentiometer that provides a dc voltage to the VCO to set the starting driving frequency. The second is a digital switch that fixes the sample point at the Nth cycle. Its setting is compared to a running count of the cycles of the driving frequency starting from the initiation of the driving tone burst. When the counts are equal, the instrument samples the filtered multiplier output, holds the voltage value, and applies it to the VCO, thus making its comparison at the end of the Nth cycle of the driving frequency. Once N is established, it must be held constant so that bolt load changes will be properly tracked by frequency changes.

Comparing the signals only at the sample point allows the operator to ignore transient effects that might be present at the start or end of the reflection tone burst. It is usually sufficient to key the sample point on a reflected signal feature such as the fifth peak to obtain the desired repeatability. It is possible that the selected signal feature might happen to lie very near the $\theta = -90° \pm 180°$ points where a little movement of the operator-set sample point might result in a lock point adjacent to the original one. A large change in the locked frequency will usually be noticed by the operator if this happens, however. The operator will also see the movement of the phase output through a half cycle if he or she is observing an oscilloscope trace of the phase output while the lock switch is thrown.

Graphically following the operation of a typical P^2L^2 system helps to clarify the frequency-time relationship. The governing action of these systems is that in the locked condition, the total number of cycles from the start of the gate to the sample point, once initially set, will remain constant as load changes. The sample point, fixed at the Nth cycle, moves in time inversely to the direction of frequency changes.

Several points should be kept in mind when following the graphical analysis. The instrument cannot change the position in time of the reflection tone burst. The travel time is governed by the physics of the situation and is not altered even as the instrument shifts its probing frequencies. The instrument begins its timing at the start of the first driving tone burst cycle sent to excite the transducer. The driving frequency then serves as the system clock for the instrument, as well as to drive the transducer. The instrument essentially counts driving frequency periods to mark signal travel time. The frequency is simply the inverse of the period.

As a bolt is loaded, changing its length and velocity, the phase-locked instrument is confronted by a change in signal travel time. Through action of the multiplier and VCO, it establishes a new frequency to relock the loop. At all locks the period of the new frequency is such that the number of periods counted between the gate and the sample point remains equal to that of the previous lock (N is held constant). The frequency corresponding to the new period length is now such that the total phase angle relationship of the new frequency to the new position in time of the reflected signal is exactly the same as that of the total phase angle relationship of the initial frequency and the initial position in time of the reflection. The new probing frequency, which is now the new system clock, has shifted just enough from the previous value to compensate

for the changed round trip travel time of the tone burst and maintain the phase lock at -90°.

Figure 3 shows phase locking response to load change as it would appear if viewed on an oscilloscope. Square wave pulses have been used for ease of providing phase information. Figures 3*A* and 3*B* are the initial reflection tone burst and driving frequency, respectively. Figures 3*C* and 3*D* are the final reflection tone burst and driving frequency, respectively.

The sample point is set by the operator prior to locking the phase lock loop, typically to coincide with a particular peak of the reflection tone burst by adjusting the initial driving frequency. Typically, the sample point is set several cycles into the tone burst to allow the signal to settle through the filter and to select an area of the signal where the multiplier output is relatively flat, corresponding better to theoretically expected output.

It should be understood that this prelock setting simply establishes an approximate lock point. It allows the operator to use a visual cue to attempt to establish a consistent lock point in future measurements. The instrument resolves the actual lock point in accordance with the previously discussed mathematical derivations. The internal count of cycles includes the number of cycles from the reflection start to the sample point in addition to the number of cycles from the gate to the first cycle of the reflection (actual travel time). The resulting lock frequency is exactly the same as it would be if the sample point were set at the first cycle of the reflection since θ is theoretically everywhere equal throughout the duration of the reflection tone burst if the driving and reflection frequencies are equal. Stated simply, the frequency satisfying $\theta = 90°$ at the start of the reflected tone burst is the same frequency satisfying it elsewhere along the tone burst.

The period count (N) shows that the lock has taken place four periods after the gate. The lock is established with the reflection signal lagging the driving signal by 90° at the sample point. The four periods come from the adjustment of the sample position by the operator prior to initial locking and the subsequent action of the phase lock loop after the operator throws the lock switch. Once established for a given measurement situation, this same relative period position must be used to relate subsequent measurements within the ±180° capture range. N must remain constant throughout the course of the measurements to maintain comparability.

Figure 3*C* shows the reflection after the bolt has been loaded. Figure 3*D* shows the new system driving frequency established by once again locking in quadrature at the final load. It can be seen in figure 3*D* that the new system frequency has once again placed the lock point exactly four cycles from the gate. Thus, as has been shown mathematically by equation 7, the frequency change becomes a measure of the travel time change. Using the scale in figure 3, the following measurements can be taken: $\Delta t/t_i$ = 1.3 μs/7.8 μs = 0.16667 and $\Delta F/F_f$ = -59,523.8 Hz/357,142.9 Hz = -0.16667. One can see from figure 3

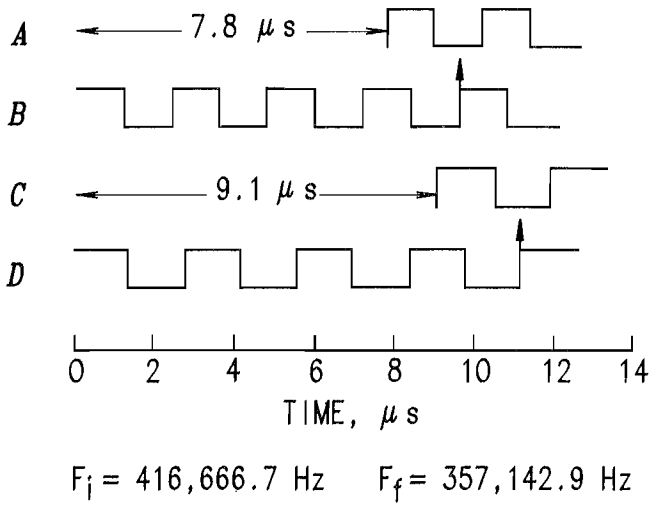

Figure 3.–Phase locking response to load change. *A*, Initial reflection tone burst; *B*, initial driving frequency (F_i); *C*, final reflection tone burst; *D*, final reflection frequency (F_f).

that the number of cycles of the driving frequency between the start and the reflection arrival always remains constant.

If F_i (416.666.7 Hz) were used in the denominator, as cautioned against in the earlier mathematical derivation, a significant error would be made. Upon further load increment this error would also be quite nonlinear. Figure 3 also illustrates the physical equivalency of the travel time measurement of conventional instruments and the period counting of P_2L_2 instruments. Figure 3 was scaled for presentation convenience, so the numbers are not typical for a mine roof bolt, however, the principle is still the same.

The difference in locked frequency that would occur in moving the sample point exactly one phase cycle to an adjacent lockpoint is give by equation 11. For typical mine roof bolts it can be calculated from equation 7, Hooke's law, and total transit time change that the instrument driving frequency should change about 775 Hz in response to a 1,000-lbf load change at about 2-MHz operating frequency. Total transit time change is about 3.6 times the time change due to the length change only. This happens because velocity changes with stress.

If the reflector distance can be chosen such that the expected total frequency change at maximum load will be less than one-half of the ΔF given by equation 11, it is conceivable that the need for visual observation could be eliminated. The operator could set the instrument to the same whole number of cycles and to the same nominal operating frequency and then switch to lock, being confident that the sample point would be within the required ±180° of the proper lock point. The reflector distance can be adjusted by employing a small hole drilled in the bolt as a reflector instead of reflecting off the bolt end. There are, however, a number of engineering tradeoffs to be made when selecting reflector distance, and some of these have a negative impact on the use of P^2L^2

technology for the mine bolt application. Long reflector distances improve accuracy but preclude eliminating the oscilloscope.

The promise of the P^2L^2 instrument lies in the relationship of its frequency measurement to time. While it is very difficult to measure the travel time of a typical 2-MHz wave to 0.00000001 s directly, it is relatively easy to measure frequency to a 1-Hz accuracy with off-the shelf electronic gear. It is, however, possible to reach a very misleading thought based on the typical frequency level and resolution. This misleading thought is that the P^2L^2 instrument has a measurement resolution of better than 1 ppm.

The 2-MHz probing frequency has nothing to do with the measurement range for a typical bolt. For a 5/8-in nominal diameter mine roof bolt, the frequency would change only about 10,000 Hz from no load to yield load. It is much more appropriate then to state that the P^2L^2 instrument has a maximum theoretical resolution of about 1.3 lbf based on a 1-Hz frequency resolution. This is still extremely good compared to alternative technologies.

The remainder of this report shows that the theoretical level was far from achievable for the actual instrument tested. A major source of this deviation of actual versus theoretical resolution was the failure of the assumption underlying P^2L^2 theory that driving and reflected frequencies always remain equal. Much of the remainder of this report documents and discusses this and other P^2L^2 technology problems. Possible solutions such as nonresonant transducers are also discussed.

RELATIONSHIP OF VELOCITY TO STRAIN AND STRESS

It should be recognized that the change in signal travel time is caused by a combination of two stress-related factors. The first factor is the actual length change from the strain. The second is the velocity change caused by the stress. The mathematical relationship can be developed using ℓ as length, t as one-way travel time, V as velocity, subscript i as initial value, and subscript f as current or final value. $\ell_i = V_i t_i$ and $\ell_f = V_f t_f$. $\Delta\ell = \ell_f - \ell_i = V_f t_f - V_i t_i$, noting that the final values equal initial values plus changes.

$$\Delta\ell = (V_i + \Delta V)(t_i + \Delta t) - V_i t_i, \qquad (12)$$

expanding:

$$\Delta\ell = V_i t_i + \Delta V t_i + \Delta t V\Delta - \Delta V\Delta t - V_i t_i, \qquad (13)$$

and $$\Delta\ell = \Delta V t_i + \Delta t V_i + \Delta V\Delta t. \qquad (14)$$

It is useful to solve equation 14 in terms of the well-known quantity $\Delta\ell/\ell_i$, which is the strain, then:

$$\frac{\Delta\ell}{\ell_i} = \frac{\Delta V t_i}{V_i t_i} + \frac{\Delta t V_i}{t_i V_i} + \frac{\Delta V\Delta t}{V_i t_i}, \qquad (15)$$

reducing further:

$$\frac{\Delta\ell}{\ell_i} = \frac{\Delta V}{V_i} + \frac{\Delta t}{t_i} + \left[\frac{\Delta V}{V_i}\right]\left[\frac{\Delta t}{t_i}\right]. \qquad (16)$$

The third or cross-product term of equation 16 is often ignored in the literature even though the equality sign is retained (*2-3*). Ignoring this term is **not justified** in high-precision measurements even though the product of two small fractional terms is very small. One can measure actual length change using instruments such as sensitive linear variable differential transformers or optical devices. Likewise total travel time can be measured with great accuracy in a laboratory setting. Performing such measurements with typical mine bolts shows that the third term of equation 16 makes up about 1% of the total value of strain with a 10,000 lbf bolt load. When the data from the P^2L^2 instrument are being combined with independent length measurements to make high-accuracy velocity measurements, or when these data are being used to study second- or third-order deformation effects, such as are sometimes modeled using Grüneisen parameters, the effect of the cross-product term is quite important and will lead to errors if it is ignored. When equation 16 is algebraically rearranged,

$$\frac{\Delta\ell}{\ell_i} = \left[1 + \frac{\Delta V}{V_i}\right] \times \frac{\Delta t}{t_i} + \frac{\Delta V}{V_i}, \qquad (17)$$

it is once again tempting to eliminate a term, since $1 + \frac{\Delta V}{V_i}$ is very nearly equal to 1. However, the other terms are also very small and the same arguments for retaining the term still hold. The error magnitude will be identical, since equation 17 is just a rearrangement of equation 16. The key to understanding here is to compare the magnitude of the terms to each other, not just to some larger number such as 1.

It is also important to examine the slight nonlinearity of velocity with stress that is evident from equation 16. The literature additionally contains implications that velocity change is linear with stress. Again this is based on assumptions that may break down if it is desired to measure very small changes. The following derivation (*6*) can be used to relate stress and velocity to a given desired degree of accuracy. The general relationship between stress and velocity for P-waves is

$$\rho V^2 = \lambda + 2\mu - \{[\lambda + 2\ell + (\ell + \lambda)(4\lambda + 10\mu + 4m)/\mu]/(3\lambda + 2\mu)\}\, T, \qquad (18)$$

where λ, ℓ, μ, m = elastic constants,

ρ = density,

V = velocity,

and T = stress.

The form of equation 18 can be seen more clearly by replacing the term in braces with a single constant, A. Then,

$$\rho V^2 = \lambda + 2\mu - AT. \quad (19)$$

Consider first the unstressed state of the material to define the initial velocity, V_o, which is the velocity when there is no stress on the material,

$$\rho V_o^2 = \lambda + 2\mu. \quad (20)$$

Subtracting equation 20 from equation 19 shows that

$$\rho V^2 = \rho V_o^2 - AT. \quad (21)$$

Solving for velocity, $V^2 = V_o^2 - AT/\rho = (V_o)^2 (1 - AT/\rho V_o^2)$, then

$$V = V_o (1 - AT/V_o^2\rho)^{1/2}. \quad (22)$$

It is not obvious at this point that the relationship of velocity to stress is nearly linear. However, if the binomial theorem is used to expand the term in parentheses, the result is

$$V = V_o [1 - 1/2(AT/\rho V_o^2) + 1/4(AT/\rho V_o^2)^2 + ...]. \quad (23)$$

From empirical measurement it is known that the change in velocity due to stress is a very small percentage of the total velocity (*7*). The AT term in equation 23 is quite small compared to the elastic constants. The terms beyond the first in equation 23 will then be very small. An approximation can then be made that

$$V \approx V_o (1 - AT/\rho V_o^2). \quad (24)$$

The value of V_o^2 from equation 20 can be substituted leaving

$$V \approx V_o \{1 - AT/(2\rho[(\lambda + 2\mu)/\rho]\}$$

$$= V_o [1 - AT/(2\lambda + 4\mu)]. \quad (25)$$

or using B to represent the constant term $A/(2\lambda + 4\mu)$,

$$V \approx V_o (1 - BT), \quad (26)$$

which shows that, within the assumptions made for the higher order expansion terms, velocity varies linearly with stress. If small changes are being measured, more terms must be retained or deviations from linearity will occur. It is not uncommon to find equations in the literature that incorrectly illustrate linear equality among strain or stress, velocity, and time or frequency terms without any mention of the approximations involved. The nonlinearity typically accounts for about 1% of the strain change for installed mine bolts. The derivations presented here also show that the direct time measurement instruments and the P^2L^2 instruments thus are measuring quantities equivalently related to stress.

LABORATORY AND FIELD RESEARCH

The preceding discussions relate mostly to the general theory of operation of P^2L^2 systems. The Bureau's research program had to deal with the implementation of the theory, however imperfect, in a real instrument. Ordinarily in mine bolt applications, the P^2L^2 instrument data are simply calibrated by relating $\Delta F/(F_i + \Delta F) = \Delta F/F_f$ directly to the load reading on a universal testing machine. This bypasses the difficulties of having to make independent measurements of all of the length and velocity parameters in equation 16. This calibration is, of course, limited to the accuracy of the testing machine, which is typically ±25 lbf, though the P^2L^2 system could theoretically resolve almost an order of magnitude better.

The majority of the laboratory experiments loaded the bolts axially, using a universal testing machine. The accuracy of the testing machine was ±25 lbf. Linear variable differential transducers accurate to ±0.00001 in were used to measure strain. Occasionally, the basic measurements were supplemented with measurements by strain gauges, load cells, and torsional loading and measuring devices.

Initially, reflections off the bolt ends were used. Later, reflectors were formed by drilling 0.040-in-diameter holes perpendicular to the bolt axis. The primary purpose of these holes was to establish a uniform gauge length because mine roof bolts are not manufactured to precision lengths. The uniform gauge length allows the calibration of one bolt to apply to a large group of similar mine bolts. Large numbers of bolts are installed for mine support. Studying the installation quality and long-term behavior of installed bolts requires that loads in a significant percentage of them be measured (*8*).

The bolts were further prepared for good transducer coupling by lathe turning their heads flat. Couplant fluid was used to further insure good coupling. Magnetic material surrounded the transducer to provide uniform coupling force.

Typical experiments produced variable results. For 1,000-lbf-load increments with probing at about 2 MHz, the change in frequency ranged from the theoretically expected value of about 775 Hz to less than a third of the expected amount. The cross-sectional area of a typical

bolt was actually less than would be calculated from the nominal diameter, but this variation was minor and did not account for the wide range of measured ΔF's. Work with travel time instruments showed that such variation was not due to any other bolt parameter variation either. Results showed the correct trend but were often not as linear as was expected. Stability testing was also begun at this time. The unit was not always stable. Sometimes when the transducer was removed and then recoupled, the new reading would be the same as the previous reading. Other times the new reading would be hundreds of hertz different.

Discussions were held with NASA representatives to try to understand and correct the problems. They suggested using a wider tone burst and setting the prelock sample point to coincide with the 5th peak of the reflection. This would insure that any time delay introduced by the loop filter would be past before lock was attempted. They also suggested that variations in couplant thickness could be responsible for the reading variations. A visit was made to NASA's Langley laboratory to conduct experiments on mine bolts. A pull test showed good linearity between load and frequency ratio though the ΔF's were about half of the expected -775 Hz per 1,000-lb load. Drift problems persisted although higher driving frequencies and different instruments were used.

Continued experiments showed that a few of the anomalous readings during tensile tests were due to slack in the load system. This was corrected by simply cycling the testing machine and the bolt to about 3,000 lbf before starting the test.

The P^2L^2 instrument allowed for the adjustment of driving frequency, tone burst width, repetition rate, and output pulse amplitude. These were experimented with to discern their effect on signal quality. Wave amplitude, wave shape, and, particularly, phase detector output could be influenced by these parameters. It appeared for given, fixed conditions that an optimum combination might exist, but finding it would require operator expertise and experimentation. It became evident that the situation being dealt with was not a simple, sinusoidal transmission and reflection situation. Transducer ringing produced more reflected peaks than there were transmitted peaks. Examination of waveforms and manufacturers' literature showed that operations were well beyond the near field focus range of the transducers. The wave path was very complex, involving multiple reflections and mode conversions. Reflections from the head and head-shank interface complicated things as well. Figure 4 illustrates a typical reflection and corresponding phase information.

P^2L^2 performance using different materials and stock shapes was analyzed. This research effort was performed to try to gain insight into what parameters affected stability and repeatability. Few trends were apparent from these experiments. The instability was difficult to pin down because its magnitude seemed to vary almost randomly.

Reflector distance experiments provided one consistent trend. When reflector distance was lengthened to about

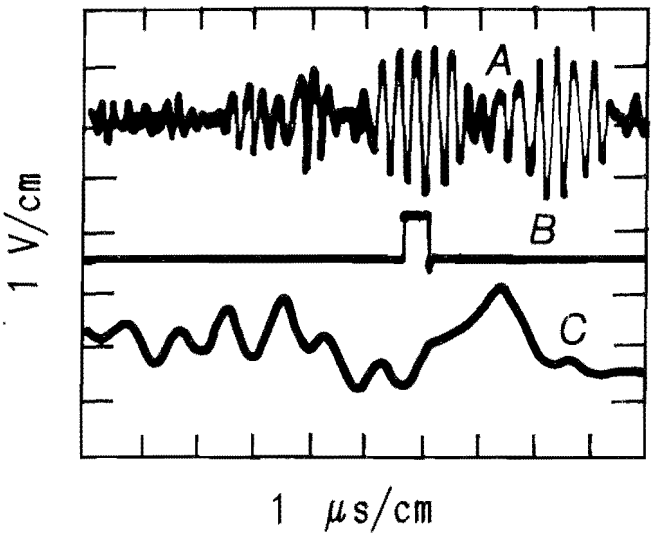

Figure 4.–Typical pulsed-phase-lock-loop signals. *A*, Reflection signal; *B*, sample point pulse; *C*, filtered multiplier output.

40 in, stability was consistently improved over that observed when reflector distance was decreased to about 5 in.Plotting the testing machine load readings against P^2L^2 normalized frequency readings sometimes produced very linear results, especially with the long reflector distances (fig. 5).

Drift problems continued to plague the device operation as more experiments were conducted. Usually the drift was within about 200 Hz, but occasionally it would run to >1,000 Hz. Because roof bolts have to be monitored over very long periods, this drift would be unacceptable as it would represent several thousand pounds load error even in the short term. The results gave some encouragement that the instrument had potential but it could not be considered field ready.

Experiments were done using shear mode transducers. There was some indication that shear waves were less subject to mode conversion. The shear transducers, however, require a thick, viscous couplant that leads to large recoupling errors because it is hard to repeat couplant thickness. The net result was that shear transducers did not offer any improvement.

Another Bureau research project was involved with a field study to determine the effects of uniform bolt tension. An understanding was developed with project and contractor personnel on this field project that the P^2L^2 system would be tried on an experimental basis only to supplement other instrumentation.

Twenty bolts were prepared with a 5-in head-to-reflector distance. Because of mode conversions and multiple reflection paths, a number of wave packets are formed. Laboratory experiments were performed to find the most stable wave packet. Laboratory readings were taken on the bolts for several weeks. Again, as the transducer was removed, then later recoupled, errors of several

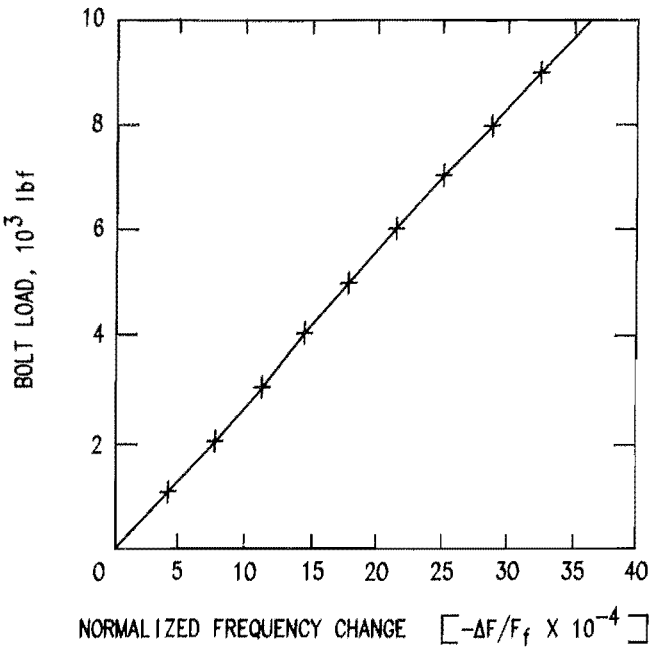

Figure 5.–Normalized frequency change versus bolt load.

thousand hertz were common even when temperature was carefully monitored to compensate the readings. Because a change of nominally 775 Hz represents 1,000-lbf load change, the readings using the P^2L^2 system at the field site were expected to have limited accuracy. By comparing P^2L^2 readings with torque readings, it was hoped that trends could at least be distinguished.

The first set of bolts was installed in an area with no ac power. The P^2L^2 instrument could not be used to take readings. This emphasized an obvious problem with the mine worthiness of the P^2L^2 technology. Power consumption of the P^2L^2 system is sufficiently high that converting to a battery-powered system would require major redesign.

The second set of bolts was installed near enough to a power center so that ac power was available. Calibration readings were taken after the bolts had reached mine temperature prior to installation. The results did show the hoped for general trends, but were far from desired accuracy goals. P^2L^2 indicated loads ranged from 2,000 to 8,000 lbf. Two bolts, which both had torque readings of 90 ft•lbf and were otherwise nominally identical, differed in P^2L^2 readings by 6,000-lbf load. Over a time period of several hours, P^2L^2 readings again indicated the expected load bleedoff trends but did not correlate well with torque readings.

In returning to laboratory work, a commercial version of the P^2L^2 instrument was purchased. A series of side-by-side comparison tests were run. It was noted that sometimes one unit would drift in one direction while the other would drift in the opposite, though both complete systems were subject to the same environment. Occasionally, both units showed very good time stability. More commonly, both units drifted in the same direction. The large recoupling errors were present with both units. These experiments showed that the nature of the drift problem was seemingly random with respect to the system electronics at least. Temperature changes alone could not be the source of the drift.

Experiments to isolate temperature effects also raised questions. Bolts were placed in temperature-controlled chambers and tested. Results were fairly consistent in showing about 150-Hz average change per 1° C at 1.5-MHz operating frequency. However, results showed that the change was nonlinear during each test. The change typically started out slowly, then increased. More confusingly, this slow-to-fast change happened whether the temperature was increased or decreased though the direction was appropriate. Temperature effects were expected to be linear because the wave path was primarily axial, and axial thermal expansion would be linear, but effects were not. Considerable data were accumulated, and log books were carefully documented. It still, however, was far from clear why the P^2L^2 unit was exhibiting the drift and recoupling errors that made it unusable.

The problems still were most often attributed to couplant thickness variation and temperature effects by those speculating explanations. Temperature was already shown to produce nonlinear effects that indicated system problems. Measuring couplant thickness directly was not possible. New comparison standards were needed to understand the problem sources.

Arrangements were made to visit the NASA Langley Research Center and conduct tests on the instrument with its developers. NASA first demonstrated the stability of the unit by placing a short bolt and transducer in a heavily insulated container and allowing everything to come to equilibrium for several hours. Subsequent readings indeed showed very high stability. NASA's conclusion from this was that the instrument itself was stable, so any drift must come from thermal change or couplant squeeze.

Tests were then made on Bureau-prepared bolts in an ordinary laboratory environment at NASA. The drift again occurred, especially with short reflector distances. NASA demonstrated that using a frequency slightly above transducer resonance would improve the phase uniformity. NASA provided adjustment suggestions, but the drift problem was still present. The fact that the drift problem remained was very important to the Bureau's research program because it established that the drift was not simply an artifact of mine bolts or of the way the instrument was being adjusted and used by the Bureau.

During these tests at NASA's laboratory, removing the transducer and then carefully recoupling it for a number of times resulted in s spread of about 270 Hz, even with the bolt mostly insulated. This would represent about a 400-lbf load error in a 5/8-in-diameter bolt. Longer term drift was also observed.

It is crucial to the understanding of this report to reemphasize that the measurement being made stems from extremely small travel-time changes. The measuring

instrument must trigger the measurement in an extremely stable and repeatable fashion. The stability must remain constant even as the bolt goes from a no-load to a fully loaded condition. To illustrate this point, consider a 5/8-in-nominal-diameter, 4-ft-long mine roof bolt. It will stretch only about 0.0006 in per 100 lbf of load. Velocity is about 231,000 in/s. The travel path is 8 ft since the wave reflects off the bolt end. Velocity reduction due to stress will increase the travel time an additional amount over that increase due to physical stretch alone, which eases the accuracy requirement somewhat. The net result is still that to resolve a 100-lbf load change, the travel time must be resolved to about 0.00000002 s. Very small system error sources can cause substantial measurement error.

IDENTIFICATION OF ERROR SOURCES

It is tempting to lump all unexpected system readings into a presumed response to thermal expansion and couplant squeeze. It is very difficult to independently measure couplant thickness change or to refute speculation that very local thermal gradients are affecting the signal path. Fortunately, the project under which these experiments were performed was set up to investigate alternative technologies to the P^2L^2 systems. Direct time measuring pulse-echo-type instruments provided a comparison with the P^2L^2 instruments.

The pulse-echo instruments allowed independent measurements of bolt strain, which would be equally affected by environment and couplant squeeze. These measurements showed that temperature effects were indeed linear. The pulse-echo instruments also showed that couplant squeeze effects were quite small. The best pulse-echo instrument could stably resolve a length change of 0.0001 in. This length change relates to a load change of about 17 lbf for a typical mine bolt with the anchor nut halfway down the threads. The 0.0001-in-length change would relate to a frequency change of about 13 Hz if the final operating frequency were about 2 MHz.

Use of the pulse-echo systems quickly showed that couplant squeeze could account for no more than ±0.0001 in, since these systems showed that both long-term stability and recoupling repeatability were within this limit. It was obvious at this point that the large magnitude and random nature of the drift problems experienced with the P^2L^2 instruments being tested could not be explained by thermal response or by couplant squeeze.

To analyze the operation of the P^2L^2 instrument further, one can develop an equation describing the physical quantity of total signal travel time in terms of instrument quantities. The sample point always lies at 360° of the last (Nth) cycle of the driving signal because it is fixed to the end of the Nth cycle by the instrument circuitry. The start of the first cycle of the reflection tone burst marks its 0° phase position. If the sample point is placed to lie within the first cycle of the reflection, there is only one point at which lock can occur, since at lock F_2 must lag F_1 by 90°. This lock will be at F_1 = 360° and F_2 = 270° in the cycle of comparison. At this lock condition the time to arrival of the reflection can then be described as

$$t_t = \frac{N}{F_1} - \frac{3}{4}\left(\frac{1}{F_2}\right), \qquad (27)$$

where the instrument is in the locked state for a given bolt load. Equation 27 clearly shows the equivalence of measuring the travel time directly and of measuring the locked frequency in a P^2L^2 instrument.

Several clues to the problem were found by the research effort. It was noted that within the limits of drift repeatability the drift magnitude was inversely proportional to reflector distance. This pointed to the multiplier and VCO phase loop circuits that deal with the fractional phase lock. The same magnitude of fractional error would become about half as significant as a percentage of total time measurement when the whole number of cycles involved doubled, as is shown mathematically in the following. Travel time with the short reflector, assuming the equal frequency case, is $t_t = (N - 3/4 + e)/f$, and with the long reflector it is $t_t = (2N - 3/4 + e)/f$, where N is the whole number of cycles, f is the lock frequency, and e is the error in quadrature lock.

The instrument could be shown to be stable when the bolt and transducer were thermally isolated and about an hour of time was allowed for the stability to be achieved. This suggested that small thermal effects on the multiplier or other circuitry were not a major problem since the instrument was kept outside the thermal insulation. It also showed that if the bolt and transducer were kept at stable temperature, the transducer position held constant, and the couplant reached a stable thickness, the electronics could maintain a stable phase lock. Changing the pulse amplitude while the loop was locked changed the lock frequency sometimes. Amplitude should not be a factor, since at the lockpoint $\cos(-\theta) = 0$. All of these observations made the actual versus ideal operation of the mixer-multiplier and filter suspect of being at least part of the problem.

The velocity of the signal waves in the bolt was then measured by using bolts of accurately measured length, counter-timers, transmitting and receiving transducers on opposite bolt ends, and an oscilloscope. This velocity can be checked for nominal accuracy using material properties handbooks. A velocity can also be calculated from P^2L^2 parameters. The whole number of cycles from the gate to the reflection reception can be read on the sample point setting thumbwheel switches. Compensation must be made for the number of cycles the sample point is set into the reflected tone burst and for the quarter cycle of quadrature lock to obtain the actual travel time to the start of the reflection. The cycle period is found from reading the driving frequency, and the round trip reflector distance is measured. As with other clues, the calculated and measured velocities generally agreed well near transducer resonance and diverged as the driving frequency moved away from resonance.

The specifications for mine bolts are well known and are detailed in ASTM F 432. Knowing such parameters as the elastic modulus and the velocity change due to stress, measuring the length change due to loads, and applying equation 27, an expected change in frequency can be calculated for a given load and starting frequency. This was done and compared with the Δf measured by the P^2L^2 instrument providing another clue to the problems of the instrument. At 2 MHz, the nominal expected value was about 775 Hz per 1,000-lbf load but values sometimes ranged down to 250 Hz per 1,000-lbf load but values sometimes ranged down to 250 Hz per 1,000-lbf load.

The puzzling nature of the instability problems was made more difficult to solve by the recommendation of the instrument builders to operate near the resonance frequency. The recommendation did make empirical sense because it would be presumed that the transducer would be most efficient at its resonance frequency. Such operation, however, hid other complex system problems because they were minimized, though not eliminated, near this resonance. The instrument builders also had shown that under the special conditions of no temperature variation, no load change, and long settling time the instrument could be made extremely stable. Still, the drift was an observable phenomenon and the clues uncovered by the research program pointed to significant system problems.

Many of the clues suggested that the driving and reflected signals were of different frequencies except at resonance. The velocity-related discrepancies could be explained, at least in part, if this were true. In compensating for the number of cycles the sample point falls into the reflected tone burst, an assumption is made that the frequencies are equal. It is evident that if the frequencies differ widely and the sample point is set the typical three to six cycles into the reflected tone burst, substantial errors could be caused since the theory is based on equal frequency. Other clues raised questions about the actual functioning of the phase-lock-loop components.

Experimental evidence suggested that combinations of the frequency differences, complex reflection signals, the amplitude sensitivities, and perhaps circuit problems caused the random and difficult to pinpoint drift problem. More detailed resolution of the causal factors required detailed analysis of the general problem of transducer resonance, fixed tone burst frequencies, and the instrument-specific problems of circuit performance.

PROBLEM ANALYSIS

The laboratory and field research effort had reached a point that clearly demonstrated there was a serious drift problem. The drift problem was very difficult to pin down because its magnitude was not repeatable from test to test, and it did not seem to have a simple, linear dependence on the factors known to influence it. The experiments with the pulse-echo direct time measurement instruments were very valuable because they established that the maximum deviation caused by the common factors of couplant squeeze, temperature effects, and transducer effects on typical bolt load measurements produced errors equivalent to only about ± 17 lbf for a 4-ft bolt. Any P^2L^2 measurements showing deviation beyond this limit must be due to causes within the measurement instrument.

The drift being nearly linear with the inverse of reflector distance suggested that within the instrument the problem likely came from the phase lock loop. The total one-way travel time for a given reflector distance is N periods plus the fractional period locked by the quadrature lock of the loop. The time, if the reflector is placed twice as far from the transducer, is 2N plus the fractional period. If there is an approximately equal instability error in the fractional period, it will be about half as significant as a percentage of time in the case of the doubled reflector distance. The fractional period is set by the phased locked loop so efforts were then focused on studying the phase lock loop in detail as it was implemented by the studied instruments.

When the research effort began to probe the sources of instability and error, it was readily apparent that the probing and reflected signal frequencies could differ widely. Further investigation showed that the reflected signal frequency was relatively constant regardless of the probing frequency. This relatively constant frequency was found to be essentially the mounted resonance of the transducer, which was the manufacturer's specified unmounted resonance frequency modified by artifacts of the mounting and environment. Problems directly related to nonidentical driving and reflected frequencies could now be explained. Additionally, this provided some further explanation of indirectly related problems because the mounted resonance can be affected by environmental and mounting factors.

The reflection signal was not only of an unexpected fundamental frequency but also was very complex. It seemed to result from a combination of signals from slightly different paths. Its shape could be altered substantially by small changes in operating frequency, bolt load, or environmental factors. In general, problems came from two major sources. The first was the resonance of the transducer, which is a general P^2L^2 problem. The second was the electronic design, which is specific to the tested instrument.

TRANSDUCER-RELATED PROBLEMS

In examining the problems related to the transducer, consider that the probing frequency also serves as the initial clock for the instrument. The sample point is set by the interval count of the probing frequency to the end of the Nth cycle. The operator chooses N by setting a digital switch. Since the start of the first cycle is fixed in time and the frequency is varied to achieve lock, the sample point does, however, move in time even though it is fixed in

position relative to the Nth cycle of the driving frequency. N must also be held constant as load changes. The time of occurrence of the start of the reflection is dependent only on reflector distance and signal velocity. It does not vary with changes in probing frequency. Prior to throwing the lock switch, there is some Δt between the sample point (end of the Nth cycle of the probing frequency) and the equivalent point in time on the nearest cycle of the reflection tone burst represented by the phase difference between the two signals. The instrument samples and holds the filtered multiplier output at the sample point time.

In the case where the probing and reflected signals are equal, multiplying the two signals together and filtering yields cos $(-\theta)$ as explained earlier in this report. θ is the fraction of a cycle that represents the time difference discussed in the preceding paragraph. As the lock switch is thrown the probing frequency will shift in response to the current multiplier output voltage, cos $(-\theta)$. The circuitry will shift the driving frequency until this voltage equals zero. When this happens, θ will equal -90° (quadrature).

θ is everywhere constant along the duration of the reflection signal in the equal frequency case for a given F_1 and N combination as shown by figure 6. The frequency that satisfies cos $(-\theta) = 0$ when the sample point is placed near the first peak of the reflection will be the same frequency that satisfies cos $(-\theta) = 0$ when the process is started with the sample point near the fourth peak of the reflection.

It is instructive to follow mathematically the actual operation of the P^2L^2 system. Because of the discrete point sampling used by the tested instrument, it is possible to accurately portray the locking sequence with step by step calculations. Both the equal frequency and nonequal frequency can be readily examined. The following section of this report examines the operation of the system starting from the ideal equal frequency case and proceeding in stages to the actually experienced case of nonequal frequencies. Possibilities of nonconvergence in certain circumstances are examined. The values used are approximately those that occur with a nominal 4-ft-long, 5/8-in-diameter mine roof bolt. For simplicity, corrections to the travel time caused by actual grip length were not made. In actual bolt installations or testing machine experiments, the

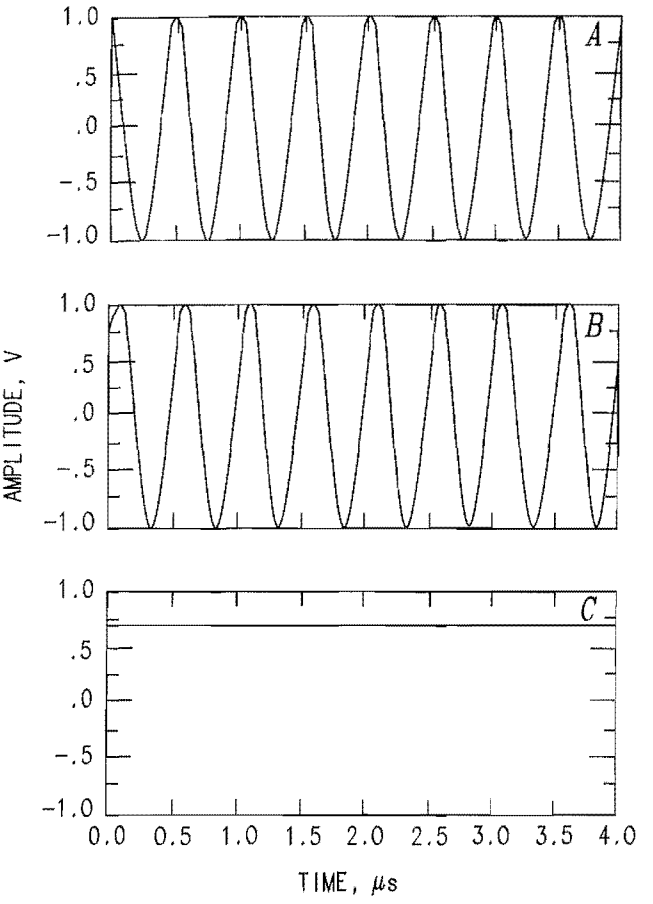

Figure 6.–Ideal mixer-multiplier output for equal frequency input. *A*, Frequency 1; *B*, frequency 2 (equal to frequency 1); *C*, mixer-multiplier output showing constant phase angle.

parts of the bolt beyond the anchor and the head flange are not subject to the full load.

The sample point is set at the end of the Nth cycle. The phase comparison then begins at the end of the Nth cycle of the driving frequency, F_1. F_1 is then always at 360° at the sample point. The governing equation at the -90° lock was shown to be $t_t = (N - 3/4)/F_1$ from equation 27 where $F_1 = F_2$.

CASE OF EQUAL FREQUENCY FIRST CYCLE LOCK

Proceeding with the examination using values typical of mine roof bolts, assume initially that N = 856 and $F_1 = F_2$ = 2,000,000 Hz. Referring to equation 27, the true round-trip travel time would be 0.000427625 s. These are the initial lock conditions.

Now assume that a load of about 600 lbf is placed on this typical bolt. The true travel time will increase by 0.000000098 s due to a combination of path length change due to strain and velocity change due to stress. Total true travel time is now 0.000427723 s.

A moment after this load is applied, the start of the reflection will have moved 0.000000098 s closer to the present position of the sample point, which is given by N/F = 856/2,000,000 = 0.0004280 s. The fractional phase angle of the reflection signal at the sample point is then (0.0004280 - 0.000427723) × 2,000,000 × 360° = 199.440°. Because the fractional phase angle of the driving frequency is always 360° at the sample point, the phase difference is 199.440 - 360 = -160.560, where the minus sign indicates the reflection signal, F_2, lags the driving signal, F_1.

The input voltage to the VCO will then be determined by cos (+160.56°), the signal amplitudes, and gain of the circuit. Because the net voltage is the gain and amplitude multiplied by the cosine value, it will be assumed that these multiplying figures are equal to 1 to simplify the discussion. This then places a voltage of -0.94299 V on the VCO. Assume that the VCO conversion factor, G, is 600 Hz/V. The frequency will change by -0.94299 × 600 Hz = -566 Hz. The new frequency for F_1 and F_2 then equals 1,999,434 Hz. This decreased frequency increases the period so the sample point, which is still fixed at the end of the 856th cycle, is now located at an increased time. To be exact, the new position of the sample point is defined by 856/1,999,434 = 0.000428121 s.

The fractional phase angle of F_1 at the sample point is still 360° because the circuitry still fixes the sample point to the end of the Nth cycle. The reflection tone burst still begins at the true signal travel time 0.000427723 s. Then at the sample point the reflection signal will have existed for 0.000428121 - 0.000427723 = 0.000000398 s. Its fractional phase angle will then be $F_2 \times 0.000000398$ s × 360°. Because $F_1 = F_2$ = 1,999,434 Hz at this point, this fractional phase angle will be 286.560°. F_2 then now lags F_1 by 73.440°. The fractional phase difference, -73.440°, now happens to be on the opposite side of the -90° lock so the lockpoint has been slightly overshot. The VCO input can again be calculated as the cos (-θ), which will now result in a positive voltage, and then the resulting output frequency can be determined. The process is repeated with the frequency converging on the final locked value as given by equation 27. Equation 27 can be rearranged, noting that in this case $F_1 = F_2$, to the form

$$F_1 = \frac{N - 3/4}{t_t}. \qquad (28)$$

From equation 28 it can be calculated that the final value of F_1 at its locked condition with the bolt under the new load will be 1,999,541.760 Hz. The circuit will continue to seek lock as described until the limits of the resolution of the multiplier and VCO are reached. The frequency display will change until its limit of resolution is reached (usually 1 Hz). Table 1 provides the results of each circuit iteration until the change in F_1 is less than 1 Hz for each new output tone burst. The final frequency value, as calculated by equation 28, will be reached within a resolution of ±1 Hz. It should again be noted that for convenience the constant gain terms involving signal amplitudes have been ignored. These terms are simply multiplied with the cos (-θ) term in the actual circuit and do not impact this discussion.

Table 1.–Equal frequency phase lock progression

θ, deg	F_1, Hz
-160.6	1,999,434
-73.4	1,999,605
-99.8	1,999,503
-84.1	1,999,565
-93.6	1,999,528
-87.8	1,999,551
-91.3	1,999,537
-89.2	1,999,545
-90.5	1,999,540
-89.7	1,999,543
-90.2	1,999,541
-89.9	1,999,542
-90.1	1,999,542

CASE OF EQUAL FREQUENCY Qth CYCLE LOCK

Proceeding from the analyses based on the sample point being placed within the first cycle of F_2 to the case where the sample point is moved several cycles into the reflection, the analysis of the equal frequency case remains largely the same. Because the periods of F_1 and F_2 are identical, moving the sample point by adjusting the whole number of cycles, N, results in exactly the same fractional phase difference, θ, that occurred during the first cycle reflection. Expressed mathematically, this statement becomes cos (-θ) = cos [-(N × 360 + θ)]. The expression for the true signal travel time now becomes $t_t = (N/F_1) - [(Q + 3/4)/F_2]$, where Q is the whole number of periods of F_2 that elapse after the beginning of the reflection.

Suppose N was increased by 3 compared to its value in the preceding paragraph in order to move the sample point over so that the phase comparison is made at a later point in time. Because $F_1 = F_2$ in this case, Q would then equal 3 and the preceding expression reduces to $t_t = [(N + 3)/F_1] - [(Q + 3/4)/F_1] = (N - 3/4)/F_1$. This is identical to the expression used in the case where the comparison was made at the very start of the reflection tone burst. Obviously, since the starting expression is the same, the remaining calculations are identical, and the frequency satisfying the locking criteria for a given load change will also be the same. This also follows from figure 6 where it can be seen that for a given value of F_1

that θ, offset phase difference, remains at the same value throughout the duration of the reflection tone burst as long as $F_1 = F_2$. It is, however, important to realize that this does not mean that θ is constant. Indeed, θ varies as F_1 varies.

CASE OF UNEQUAL FREQUENCY QTH CYCLE LOCK

The unequal frequency situation is considerably more complex to analyze because the net phase difference depends on several variables, some of which have nothing to do with the physics of the loaded bolt. Now the net phase difference depends not only on the offset angle, θ, but also on the ωt terms in equation 9. This net phase difference angle will be called θ_N. The net phase difference at some increased value of N will depend not only on the initial offset but also on the relative phase change between F_1 and F_2 caused solely by their differing frequencies. This relative change obviously changes the frequency that will satisfy the lock condition, but it is unrelated to the bolt load change. For the same load change then, there will be different values of F_1 at lock depending on which cycle the sample point is placed at in time.

In the equal frequency case, the net phase difference of the reflection tone burst and the continuation of the driving signal were dependent only on the offset, θ, caused by the physics of the signal travel path. For a given offset, θ stayed the same whether the signals were compared at the start of the reflection tone burst or at any other point along the duration of the overlap of the two signals. However, in the unequal frequency case, θ no longer constitutes the entire makeup of the net phase angle difference between the two signals.

Recall that the general form of the filtered multiplier output was $1/2\ M_1M_2\cos(\omega_1 t - \omega_2 t - \theta)$. Time, t, here begins at the first arrival of the reflection tone burst and runs to the point at which the signals are being compared (the sample point). It will subsequently be referred to as t_r. The VCO still receives a voltage signal that is still represented by a cosine function. The locking process will still occur when the cosine function equals zero at 90° net phase difference. Now, however, the phase difference angle is formed by the ωt terms as well as by the initial offset θ. In general then, θ will not equal -90° at lock except at odd instances when the ωt terms happen to exactly equal multiples of 360°. At lock, the entire angle quantity will always still equal +90°.

To continue the analysis, a new term, M, needs to be defined. M is the number of the cycle of F_1 that would place the sample point within the time frame of the first cycle of the reflected signal. Once the sample point is moved into the overlap zone, M will not equal N. M is needed to calculate the value of the initial offset, θ. Using M, previously defined terms, and realizing that F_1 is at 360° at the end of the Mth cycle, and that the phase of F_2 at the start of the reflection is 0°, an equation for θ can be written

$$\theta = 0° - \left[360° - \left(\frac{M}{F_1} - t_t\right) \times F_1 \times 360°\right]. \quad (29)$$

The term in parentheses quantifies the time gap between the end of the Mth cycle of F_1 and the beginning of the reflection tone burst. Multiplying this time gap by F_1 converts the time to an equivalent phase amount so subtracting from 360° gives the phase of F_1 at the start of F_2.

An equation for t_r can be developed relating it to previously defined terms.

$$t_r = \frac{N}{F_1} - t_t. \quad (30)$$

This equation quantifies the amount of time the signals are overlapped at the sample point time starting from the beginning of the reflection.

Substituting these quantities into the angle expression and realizing that at lock the net phase angle will equal 90° or some multiple of 360° plus 90°,

$$0 = \cos\left\{(360° \times F_1 - 360° \times F_2) \times \left[\frac{N}{F_1} - t_t\right] + \left[360 - \left(\frac{M}{F_1} - t_t\right) \times F_1 \times 360°\right]\right\}. \quad (31)$$

All of the quantities in equation 31 are fixed by the operator settings and the analysis assumptions except F_1 and M. That is, if N is again set to 856, if t_t initially is again fixed to 0.000427625 s by the travel path, and F_2 assumed to be constant at transducer resonance of 2,500,000 Hz, then the value of F_1, which will satisfy the locking criteria, can be found.

Recalling the definition of M, the following expression can be written

$$M = \text{Integer}\ (t_t \times F_1) + 1. \quad (32)$$

It can now be seen how the direct solution for this unequal frequency, overlapped case begins to get complex. To reach a solution of equation 31 for F_1, the value of M must be known. However, determining the value of M requires that the value of F_1 be already known. Because this is not possible, an estimate of the value of F_1 must be used to calculate M using equation 32. This value of M is then inserted into equation 31 to calculate F_1. This calculated value of F_1 is then used in equation 32 to calculate M and see it matches the original estimate. If not, the estimate of M is revised, based on the difference of the two estimates and reinserted into equation 31. This iterative process must continue until an exact match is found so F_1 satisfies both equations. Fortunately, the process is aided by knowledge of the equal frequency case and by the fact that F_1 in equation 32 can be initially misestimated significantly and still yield the proper integer value of M. A good initial estimate of F_1 can be found by using F_1 calculated as in the equal frequency case.

The situation becomes still more complex because equation 31 is not convertible into a simply soluble form. In earlier discussions, the ωt_r portions of the angle dropped out because the frequencies were equal. Now their contributions must be considered. θ is always less than 360°. However, there is a possibility that $\omega_1 t_r$ will yield a quantity larger than 360° depending on the value of t_r and the magnitude of the frequency gap. The locking criteria of the cosine, being equal to zero and decreasing if the angle increases, are met by the angle being equal to 90° as well as 90° + L × 360°, where L is an integer. Thus, the general solution of equation 31 must allow for the periodic repetition of solution points. Earlier, the equations could be simplified by knowing that the angle had to be equal to 90° at lock. Now it is only known that the angle will equal 90° + L × 360°. Additional complexity has been introduced once again because L also depends on the value of F_1, which is not known prior to solving the main equation. Again, an iterative process must be used.

$$L = \text{Integer}\left[\frac{360\ F_1 t_r - 360\ F_2 t_r}{360}\right]$$

$$= \text{Integer}\,[F_1 t_r - F_2 t_r]. \qquad (33)$$

Substituting the value of t_r from equation 30

$$L = \text{Integer}\left[F_1\left(\frac{N}{F_1} - t_t\right) - F_2\left(\frac{N}{F_1} - t_t\right)\right]. \qquad (34)$$

The same estimate of F_1, using its value from the nonoverlapped situation, provides a good starting estimate of L.

A soluble equation derived from equation 31 can now be written since it is known that the net angle quantity inside the cosine function must equal +90° + L × 360° at lock.

$$+90° + L \times 360° = (\,360° \times F_1 - 360° \times F_2\,) \times \left[\frac{N}{F_1} - t_t\right]$$

$$+ \left[360 - \left(\frac{M}{F_1} - t_t\right) \times F_1 \times 360°\right]. \qquad (35)$$

Expanding equation 35 and combining terms leaves

$$+\frac{1}{4} + L = N + F_2\left(t_t - \frac{N}{F_1}\right) + 1 - M. \qquad (36)$$

Equation 36 shows that the solution will be complex because two quantities, L and M, must be estimated. L and M both depend on F_1. Substituting all of the values into equation 36 leaves the expression

$$+\frac{1}{4} + \text{Integer}\left[F_1\left(\frac{N}{F_1} - t_t\right) - F_2\left(\frac{N}{F_1} - t_t\right)\right] = N$$

$$+ F_2\left(t_t - \frac{N}{F_1}\right) + 1 - \text{Integer}\,(t_t F_1 + 1). \qquad (37)$$

Fortunately, the situation is well defined physically and knowledge of the equal frequency case can be used to establish initial F_1 estimates.

Getting a solution is relatively formidable in terms of the number of calculations that must be made. There are two tiers of iteration because of the need initially to estimate L and M.

The dual-tiered iteration might become extremely cumbersome if M and L were independent and not bounded. It is evident, however, that since both depend directly on F_1, there is a relationship between the two. However, there is not a simple, soluble relationship between the two, but by exploring the limits of F_1 to preserve a given estimate of M without moving to the next higher or lower integer, bounds can be placed on L.

The upper and lower values of F_1 are placed into equation 34, which sets limits for L. In a computer program L is then incremented from its lowest value from the preceding process to its highest value. If no satisfactory solution of F_1 that also causes the value of M to match its original estimate is found in this range, then M must be incremented. Also, since the operator sets the total number of cycles duration of the tone burst, bounds can be established on M. Its highest possible value is equal to N. This presumes that the operator has set N somewhere in the signal overlap zone. This is reasonable since the circuit would never lock otherwise. In extreme situations it might be necessary to extend the range a few cycles to allow for the reflection tone burst being longer than the set value because of transducer ringing.

Depending on the situation, one might find it easier in this case, where F_2 is fixed, to examine lock points by mathematically modeling the circuit, using equation 29, and guessing at initial F_1 values. The initial lockpoint can be readily found since at lock $360 \times F_1 \times t_R - 360 \times F_2 \times t_R - \theta = 90$. One proceeds as before after loading by calculating the net phase difference for the load-induced time change. Frequency change is, as before, equal to the VCO factor, G, times the cosine of minus the net phase difference. The only thing different is that F_2 remains fixed. It no longer changes in tandem with F_1. Lock will then be different than it was in the case where F_1 and F_2 always remained equal. The travel time remains the same since it is fixed by the physics of the travel path.

To keep the equation balanced F_1 has to change compared to its value in the equal frequency case. If t_t = 0.000427625 s, N = 856, G = 400 Hz/V, and F_2 is assumed constant at 2,500,000 Hz, the initial lock frequency, F_1, will be 2,000,351 Hz. Note this differs

substantially from the equal frequency case where F_1 equalled 2,000,000 Hz. This difference occurs even though the sample point is still placed within the first cycle of F_2. If an approximately 600-lbf load is placed on the bolt so t_t again equals 0.000427723, then a final locked frequency of 1,999,893 Hz will be reached as shown in table 2. θ_R is the net phase angle difference of F_2 compared to F_1. It is composed of both the initial offset and the time-dependent terms.

Table 2.–Unequal frequency phase lock progression

θ, deg	ωt, deg	θ_R, deg	F_1,Hz
-214.6 . . .	-36.3	178.3	1,999,951
-153.0 . . .	-51.8	101.2	1,999,873
-141.0 . . .	-54.8	86.2	1,999,899
-145.1 . . .	-53.8	91.3	1,999,890
-143.7 . . .	-54.1	89.6	1,999,893
-144.1 . . .	-54.0	90.1	1,999,892
-144.0 . . .	-54.0	90.0	1,999,893

The unequal frequency situation, which is reflective of the actual instrument, dramatically alters the lock points. The difference in three-fourths of a cycle of F_2 in the equal and nonequal cases is a very small quantity of time. Once again, because very small changes in time are being measured, the difference is highly significant. In the illustrated case it alters the initial lock frequency by 351 Hz. More importantly, the theoretical relationship $\Delta F/F_f = \Delta t/t_i$ no longer holds. The time change and the initial time, of course, have remained the same. ΔF has stayed nearly the same. F_f has, however, changed considerably.

The change in $\Delta F/F$ is small enough that when working within ±50-lbf-accuracy limits, it might not be noticed. It will fall within the error produced by rounding off the lock frequency to 1 Hz. If high-precision measurements are being made, the artifact effect of unequal frequencies could have a major impact. If the absolute values of F are being used in calculations, the effect would also be of major significance. A most critical consequence of unequal frequencies is that the output of the multiplier will now be a sinusoidal signal rather than a straight line. The circuitry of a P^2L^2 instrument does not perform any intelligent analysis. It simply locks when the voltage reaches zero. As the analysis proceeds to the more typical case of the sample point being placed to coincide with the third cycle of the reflection, the impact of this unequal frequency effect will be shown to grow considerably.

If the sample point was placed three cycles into the reflection tone burst (N = 859), the initial lock would now be 2,001,747 Hz and the final lock 2,001,291 Hz, as shown in table 3. Note the ωt terms in table 3 can cause a phase shift of more than 360° so the whole cycle would need to be subtracted to separate the 90° quadrature lock from the whole number of cycles. Note now that the lock frequency differs from the equal frequency case by 1,749 Hz.

In general, this modeling technique might prove easier to use than the first solution. The initial estimates of F_1 at lock can be very rough. If the solution does not lock, then a new estimate is tried. The model converges very rapidly, so many tries can be made in a very short time.

Table 3.–Third cycle, unequal frequency phase lock progression

θ, deg	ωt, deg	θ_R, deg	F_1, Hz
-69.5	-251.8	-182.2	2,001,347
-8.0	-267.1	-259.1	2,001,272
-356.3 . . .	-270.0	86.3	2,001,298
-0.3	-269.0	-268.7	2,001,289
-359.0 . . .	-269.4	89.6	2,001,291
-359.4 . . .	-269.3	90.1	2,001,291
-359.3 . . .	-269.3	90.0	2,001,291

Note.–F_2 = 2,500,000 Hz.

OSCILLATION CONDITIONS

There is a potential problem in P^2L^2 circuit design that should be recognized. It became apparent when circuit behavior was modeled on a computer. The step-by-step adjustment of VCO input voltage is dependent on a cosine function. The cosine function has several points of positive to negative symmetry, one of which is at the -90° lock point. It is possible then to have a situation where the frequency adjustments become symmetrical about the lock frequency, and the loop gets stuck oscillating between two values. Expressed mathematically, the situation becomes

$$F_j - F_{90} = F_{90} - F_{j+1}, \tag{38}$$

where F_j and F_{j+1} are the frequencies at successive interations.

In general, anytime the VCO conversion factor, G, is large enough to cause a correction to overshoot the -90° lock point from the opposite side, oscillation is a possibility. The exact condition for causing oscillation can be found by noting that $F_{j+1} = F_j + \Delta F$ and developing equation 38 further to show that at oscillation

$$\Delta F_c = \left| 2 \times (F_{90} - F_j \right|. \tag{39}$$

The subscript c indicates the minimum critical value to cause oscillation. When the condition of equation 38 is met, the circuit can adjust between F_j and F_{j+1} indefinitely because of the symmetry about the lock point.

Analyzing the critical value of ΔF requires remembering that the sample point is always at the end of the Nth cycle of the driving frequency. That is, the phase angle of the driving frequency is always 360° at the sample point time. The phase angle of the reflection frequency is defined by the amount of time it has existed from its start to the sample point multiplied times its frequency. Subscript R indicates reflection.

$$\gamma = \left(\frac{N}{F_D} - t_t \right) \times F_R \times 360, \tag{40}$$

γ is the reflection signal phase angle, t_t is the true travel time, and subscript D refers to the driving signal. For ease of analysis, presume that the frequencies are equal as before and that the sample point is placed within the first cycle of the reflection.

Additionally, assuming the jth iteration of adjustment, equation 40 can be algebraically rearranged to yield for the equal frequency case

$$F_j = \frac{N}{t_t} - \frac{\gamma}{360t_t} = \frac{360N - \gamma}{360t_t}. \quad (41)$$

The phase difference θ is always equal to γ - 360 because the sample point is always at 360° phase angle of the driving frequency. Then making this substitution, calculating F for the θ = -90° lockpoint, and substituting into equation 39

$$\Delta F_c = 2 \times \left(\frac{360N + 90 - 360}{360t_t} - \frac{360N - \theta_j - 360}{360t_t} \right)$$

$$= \cos\theta_j \times G. \quad (42)$$

Solving equation 39 for the critical VCO conversion factor, G, at oscillation

$$G = \left[2 \times \left(\frac{+90 + \theta_j}{\cos\theta_j \times 360t_t} \right) \right]. \quad (43)$$

There is obviously a solution for G for each possible θ_j. The need is to find the lowest G value that will cause problems and design the circuit to stay below it. First, t_t is set to the highest expected travel time, then it remains to find a minimum for the quantity $(+\theta + 90/\cos\theta$. At θ = -90° the quantity becomes minimized but not defined in a useful manner. As -90° is approached, a useful minimum is reached because the value of this term changes very slowly. The value of the angle terms approaches about 57.3. Combined with the travel time this value determines the critical G. If oscillation occurs below this level, it will not be of concern because the frequency readout will not change. For a typical mine roof bolt situation, a critical G is about 766 Hz/V. Table 4 shows the oscillatory pattern that develops if the situation is the same as in table 1 but G is increased above the critical value to 780 Hz/V.

In practice there will normally be enough instability in the circuitry, the temperature, and the load to prevent a long-term oscillation, but a user should be aware of the effect. It might cause long convergence times even if the oscillation is not permanent.

In general, there is an inverse tradeoff of convergence time with nearness to oscillation of the VCO convergence factor. Because the tone burst usually repeats hundreds of times per second in typical mine bolt situations, this is not normally a problem. It might become a concern if the P^2L^2 unit were being used in a real-time installation torque control application. For a continuous load, the high repetition rate assures that the incremental phase output voltage change will be small so it is unlikely that a problem would occur. In a remeasurement situation, however, the operator could easily place the prelock sample point as much as 180° away from its final value, so a problem could occur.

Table 4.–Oscillation of the phase lock progression

θ, deg	F_1, Hz	θ, deg	F_1, Hz
-160.6	1,999,265	-120.7	1,999,343
-47.3	1,999,794	-59.4	1,999,740
-128.8	1,999,305	-120.6	1,999,344
-53.6	1,999,768	-59.5	1,999,740
-124.9	1,999,322	-120.5	1,999,344
-56.2	1,999,756	-59.5	1,999,739
-123.0	1,999,331	-120.4	1,999,345
-57.6	1,999,750	-59.6	1,999,739
-122.0	1,999,336	-120.4	1,999,345
-58.4	1,999,745	-59.6	1,999,739
-121.4	1,999,340	-120.4	1,999,345
-58.9	1,999,743	-59.6	1,999,739
-121.0	1,999,342	[1]	[1]
-59.2	1,999,741		

[1]Last 2 values repeat endlessly.

The instruments that were tested used a very large VCO conversion factor. Ordinarily this would have swung the ΔF amounts so much that the circuit would have jumped to adjacent lockpoints and perhaps never properly locked. The mixer-multiplier output was so nonideal, however, that it contained small ripples and was shaped so that the ΔF swings were kept in bounds. The limited slew rate of the VCO also helped keep these overly wide swings from occurring. In general, one should be aware of the potential for oscillation and design the VCO conversion factor to always be low enough to avoid it.

CASE OF UNEQUAL VARIABLE FREQUENCY LOCK

The previous analyses are based on F_2 at least being constant. In fact, the value of F_2 was very fragile and variable in actual experiments. Table 5 presents a set of measured F_2 values, as F_1 was varied. The value of F_2 was determined by using an oscilloscope and counting zero crossings of the center six cycles of an eight-cycle tone burst. The table provides the fundamental frequency present, but it should be understood that the F_2 waveform is complex.

Table 5.–Reflection frequency (F_2) dependence on driving frequency (F_1), hertz

Driving	*Reflection*
1,959,143	2,000,100
1,754,813	1,960,784
1,505,806	2,898,550
1,249,961	2,191,780
1,005,048	3,000,000
930,359	3,000,000

The F_2 waveform is a combination of the mounted transducer resonance, various harmonics and other physical resonances, interference between wave packets that have traveled slightly different paths through the bolt, and mode converted waves. It is not a simple, single-frequency sinusoid. The reaction of the instrument to this waveform depends on the interaction of the mixer and the multiplier with all of the frequencies present.

To have no effect on measurement stability, the relationship of F_2 to F_1 would have to be precisely defined and repeatable. The patterns shown by table 5 show instead a relatively random relationship.

The data in 5 were obtained from tests with a 4-ft-long typical mine bolt. The driving frequency measurement is accurate to ±1 Hz. The reflection frequency was measured by reading the period of the fundamental frequency from an oscilloscope trace. The reflection frequency measurement accuracy is about ±3%. The reflection waveform is complex, but the fundamental provides a measure of what the filtered multiplier output should contain. The repeatability of the reflection frequency was about ±20%. Slight variations in couplant thickness, transducer position, and temperature would alter repeatability. The general trend was, however, repeatable. It shows how nonideal the actual transducer behavior was. The nominal unmounted resonance of the transducer used in compiling table 5 was 2.25 MHz.

The value of F_2 seems to be governed primarily by mounted resonance but table 5 shows that other factors can cause substantial variations about this point. Generally the variation worsens as divergence of driving frequency from resonance frequency increases. Sometimes as F_1 decreases, F_2 decreases, and other times the opposite relationship is shown. The pattern is not uniformly cyclic. Repeated measurements also showed that the values were only repeatable in terms of gross trends. The fundamental frequency of F_2 probably varies as the mounting and environmental factors vary. F_2 varies as bolt dimensions change during loading, as well. Transducer position has pronounced effects on F_2 wave shape. Change in the wave shape would likely cause the instrument to adjust by changing locked frequency.

Directly measuring variations in F_2 on the order of 3% or less during actual load measurements was not possible. The reflection tone burst exists for only about six cycles of a ≥1-MHz signal. The effect of F_2 variation on the measurement is, however, seen as variations of the locked frequency, F_1, that occur without bolt load change. These variations also explain why P^2L^2 instruments overreact to changes in parameters such as temperature and transducer position.

The effect of F_2 variation on the locked frequency is diminished by the fact that any change in reflection tone burst period for perhaps a total of six cycles of F_2 is compensated for by change in F_1 period that occurs over N cycles. The per cycle change will then be divided down by about 6/N. Nevertheless, a relatively small percentage variation of F_2 can have an effect on the locked frequency that is very significant in terms of the desired load measurement. A few hundred hertz variation in the locked frequency is equivalent to about 300 lbf of load change. Even a 0.05% change in F_2 causes a noticeable change in F_1.

Such variations in F_2 explain most of the instability and drift problems that were observed while testing P_2L_2 instruments. These variations are believed to be generic to all similar instruments and transducers. Numerous types of transducers were used during the course of the research. Various commercial transducers and types of tone burst sources were used. The results were always similar. To avoid the problem, a transducer that did not exhibit resonances would have to be found. Even then the effects of multiple travel paths might still be present.

To get high-amplitude signals and maintain uniform reflector distance, 0.040-in-diameter reflector holes 15 in. from the bolt heads were typically used during the research. Because N would be less than a third as large compared to the 4-ft case, the effects of variations in F_2 would be multiplied by more than three, because the value of 6/N would be tripled.

The preceding discussion also explains why, under the special circumstances of setting the probing frequency very near to the mounted resonance frequency, holding temperature very constant, and keeping transducer position constant the P^2L^2 instruments appear very stable. Simply rotating the transducer slightly, however, will produce changes in the lock frequency far exceeding the equivalent changes produced when using a pulse-echo instrument. Similarly, changes in any other factors controlling mounted resonance or wave shape will cause significant unwanted lock frequency change.

The influence of any absolute fractional phase error is related to the total load measurement as a percentage. Use of long reflector distances could reduce absolute load error magnitudes to possibly acceptable levels where such lengths are possible. The fractional phase errors would still be present at the same absolute levels and the operator should always be aware of them. Where reflector distances are short (< ~ 24 in), the impact of the phase error on the load value will usually be high.

The relative accuracy of P_2L_2 instruments related to reflector distance bears some further examination. It is evident that total time and time change both double if reflector length is doubled and the load is held constant. Strain ($\Delta\ell/\ell$) stays constant if gauge length is doubled while load is held constant. For a given time resolution capability, the load could be measured to an uncertainty half as large with the longer reflector distance since the small time change is the factorlimiting accuracy. Because the maximum driving frequency was limited to about 2 MHz by the principal P^2L^2 system tested, the same driving frequency would normally be used for both situations.

If F_f is held nearly constant, then ΔF must remain nearly constant. The observed change in frequency will be the same regardless of bolt or reflector length. One might incorrectly infer that the accuracy of the measurement relating $\Delta F/F_f$ to load is then constant. In the case of a short reflector, N cycles of F_f are used to measure the signal travel time. The load change will cause a travel-time change represented by a fraction of a cycle. In the case of a long reflector, the load causes double the amount of travel-time change. This doubles the fraction of a cycle representing the change. For a given fractional phase resolution capability then, the uncertainty in the load measurement is halved for the longer length. The P^2L^2 instrument can be thought of as simply marking time by counting whole and fractional cycles.

Some efforts were made to explore minimizing or eliminating the tendency of the transducer to drive at resonance-related frequencies rather than at the desired

driving frequency. It was found that even when smooth sine waves that were switched on and off near zero crossings were used to drive the transducers tested, they still oscillated at mounted resonance when driven by tone bursts. Reference 9 gives some indication that it is possible to build a nonresonant transducer by properly shaping the crystal. There would probably be significant tradeoffs in transducer efficiency, however. The effects on reflection frequency of harmonics of the bolt resonance and of the reflection being a complex combined waveform might still cause some problems, even with a broadband transducer. Exploring such a solution was beyond the scope of the mine bolt research because a suitable alternative technology of pulse-echo measurement was found.

Finding a solution to transducer resonance problems seems to be the largest barrier to developing a P^2L^2 measurements system that is stable under all conditions. Unless the frequency relationship of the driving and reflected tone bursts can at least be held constant, the P^2L^2 technique cannot be made consistently stable. Unless the driving and reflected frequencies can be made always equal, the performance of the P^2L^2 system cannot be related to the generally applicable mathematical theory yielding a linear relationship between frequency change and load change.

There was some suggestion during the course of the research by instrument builders that using multiple reflectors and observing only the changes in the time or phase between them would solve instability problems. This technique might eliminate the effects of legitimately measured variation of the couplant thickness from the measurement, but these effects were shown by the pulse-echo instrument to be insignificant. Some instability problems and nonconformance to theoretically expected output would still be present because the signal paths, amplitudes, and reflection wave shapes would be different and part of the change would still be due to randomly varying factors unrelated to load change.

A variety of ultrasonic transducer models from different manufacturers with a variety of nominal resonances were used. These included those suggested by the builders of the tested P^2L^2 instrument. All oscillated at a frequency primarily determined by their mounted resonance, not their driven frequency.

The preceding discussions of transducer resonance would apply to any P^2L^2 instrument using such transducers. An additional problem source observed, which was related to the electronic design of specific instruments tested, is discussed in the following section.

INSTRUMENT-SPECIFIC PROBLEMS

Figure 7 provides a schematic of the specific components of the phase-lock-loop in the NASA-built instrument. The operation starts with the digital VCO generating a probing frequency. This frequency is fed to three different subcircuits. It forms the time base, which counts the whole number of cycles and produces the sample point signal at the end of the Nth cycle. It is amplified and becomes the driving frequency. The VCO frequency is also fed to one input of the doubly balanced mixer-multiplier.

The VCO is a digital device producing a unipolar square wave. This makes interfacing to digital devices, such as counters, easy, but also introduces spurious frequencies associated with its complex form into the analog multiplier circuitry.

The transducer senses the returning reflected tone burst. This reflected tone burst, which has been twice filtered by passage through the transducer, is then fed to the other input of the mixer-multiplier. The output of the mixer-multiplier is ideally a voltage proportional to the product of the two inputs. The product voltage signal then passes through a buffer amplifier to a low-pass filter that removes the high-frequency components from the signal. For the 2- to 3-MHz probing frequencies used in these experiments, the filter rolloff is typically set to 1 MHz. This level is set to elimnate the sum frequencies as shown by equations 9 and 10.

The filtered product voltage is then fed to the sample and hold (fig. 7). The control input of the sample and hold is the sample point pulse. Prior to closing the lock switch, the operator sets the sample point pulse by visually observing the reflection and moving the sample point position in time by adjusting the whole period count thumbwheel switches and by tuning the driving frequency. The sample and hold captures the filter output and then feeds the voltage from the filter at the sample point time back to the VCO, thus completing the loop. The filtered voltage represents the difference between the starting phase difference and θ = -90°.

If voltage is less than zero, the frequency of the VCO will decrease and vice versa. The multiplied voltage signal will again be sampled after the next gated tone burst has occurred, the reflection has traveled back to the transducer, and the sample point time is again reached. The process will repeat until the sampled voltage equals zero, which, in theory, is at the type of transition point shown in figure 2. If the driving signal and the reflected signal are simple sinusoidal signals equal in frequency, this is equivalent to making the phase difference equal to -90°. The action of the phase-lock-loop would then find the quadrature lock nearest to the sample point.

Explaining the specific problems of the instrument requires close examination of the ideal and real behavior of the mixer-multiplier and the filter. The analysis of the mixer-multiplier and filter is specific to the particular instruments that were tested. It may or may not apply to other instruments since it depends on specific circuit components and hookups.

Ideally, the multiplier would produce an output that would be equal to a simple point-by-point multiplication of the two input signals. Typical mixer multipliers, however, rely on rather indirect analog techniques. They are used primarily in circuits such as radio transmitters and receivers where a high-frequency carrier is modulated by a lower frequency information signal. a mixer is used to combine the signals at the transmitter and to separate them at the

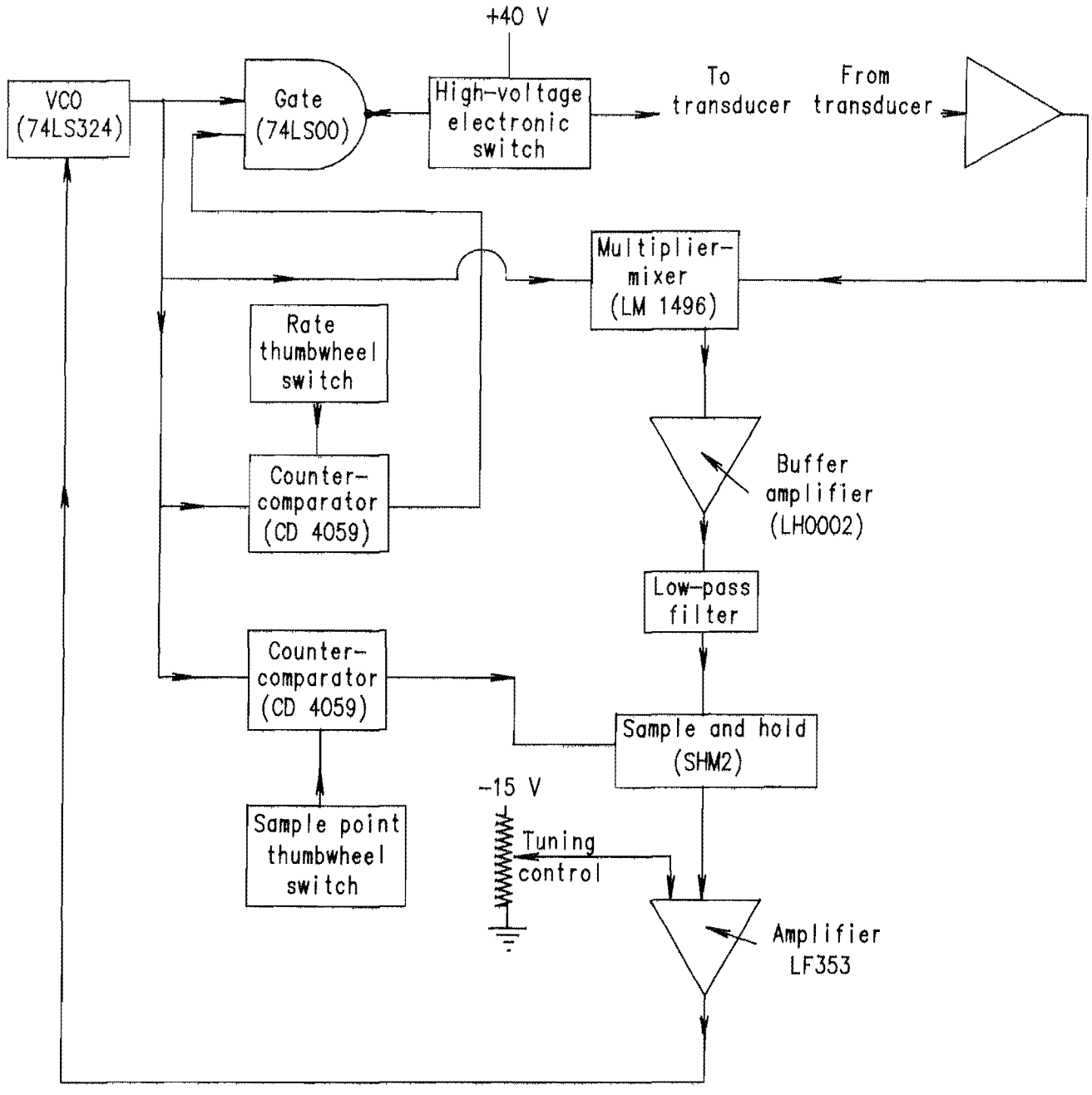

Figure 7.–Pulsed-phase-lock-loop instrument electronics.

receiver. The mixer typically has three ports. One is the high-frequency input called the local oscillator port (L). Another is the low-frequency input called the received frequency port (R). The third is the output called the intermediate frequency port (I).

The L and R frequencies are mixed by placing them across common diode semiconductor junctions. The switching action of the junctions, combined with their nonlinearity, is used to create an output that contains the desired sum and difference frequencies (*10-11*). The output also contains all of the possible undesirable intermodulation products, such as $\pm mF_2 \pm nF_1$, where m and n are integers. The intermodulation products can combine with the original frequencies to produce multiple tone intermodulation products as well. Combinations of the input signal power levels relate in a complex way to the power levels of the undesirable output products.

Additional diode junction components are often added to help suppress undesirable output products. These are arranged so that many undesirable products at least

partially cancel. The industry standard is the doubly balanced mixer. Double balanced mixers theoretically generate only one-fourth of the possible intermodulation products, but this depends on component tolerance and match.

Consider the complex action of a diode junction used in a mixing application. The nonlinear current-to-voltage relationship provides mixing, and switching (reverse bias) also provides mixing as the L port signal oscillations alternately forward and reverse bias the junction. The actual mixing is a result of the combination of these two mixing sources. The nonlinearity mixing can be described by approximating the diode current by

$$I \cong I_o\, e(\cos\omega_1 t + \cos\omega_2 t)/V, \qquad (44)$$

V is the thermal noise-induced voltage and I_o is the reverse bias saturation current. This equation can be expanded in a power series of the form

$$I = I_o \sum_{N=O}^{N=\infty} \frac{(\cos\omega_1 t + \cos\omega_2 t)N}{V^N\, N!} \qquad (45)$$

A DC term is formed at N = O, the fundamentals are formed when N = 1. When N = 2, the second harmonics plus the desired sum and difference frequencies are formed. Higher order intermodulation products appear with increasing N.

Next consider the switching action between full forward bias and full reverse bias. The switching action is caused by the comparatively large L port signal. The R port signal then is simply gated through, or not gated through, to the I port, depending on whether the switch is open or closed. Consider the switching signal as an odd harmonic square wave. A Fourier series describing the gated sinusoid at the I port (output) could then be written. All of the harmonics of the switching signal multiply with the sinusoid at the R port to form intermodulation products of the form $\cos(N\omega_1 t)\ \cos(\omega_2)$ where N is an odd integer. Because the actual diode junction does not switch instantly, but moves through its nonlinear region for a finite time, the I port output of a real mixer is a combination of the two sources described. Further details of mixer operation can be found in references on the subject, such as references 10 and 11.

From the preceding discussion it is evident that the mixer operation is complex. DC bias levels and signal power levels can obviously be critical to circuit operation. A given mixer might be optimized for certain conditions, but it will have a finite dynamic range where desired operation will occur. The upper level of the dynamic range is considered to be the compression point at which the I port power change falls 1 dB below the R port power change as R port power is incremented. The lower level is set by the noise level of the mixer as installed in the system.

An important figure of merit is the measure of the suppression of undesired intermodulation products. A key contributor to this figure is L port to I port isolation. Another important figure of merit related to intermodulation suppression is the intercept point. This is the level of R port power at which the power of the undesirable products and the desirable products at the I port would be equal. This is an extrapolated figure, because the compression would reduce I port power before the intercept point would be reached. All of these related factors are discussed at least briefly here to convey that selection of circuit components and operating levels is critical to obtaining the desired operation for a given measurement situation.

The instrument builders chose to use an integrated-circuit double-balanced, commercially available modulator-demodulator (LM 1496). It is designed for typical radio-frequency modulation and demodulation where the L port input is expected to be high frequency and the R port a much lower frequency. The L port has a bandwidth of up to 100 MHz. The R port, however, begins to roll off by 2 MHz. Because the roof bolt application uses transducers with resonances of 2.25 MHz and higher, the choice of the LM 1496 seems questionable, just for the 2-MHz rolloff. It was not possible to determine all of the previously discussed figures of merit for the LM 1496 from the manufacturer's literature that was readily available to the author. Breadboarding circuits using an isolated LM 1496 did, however, show that dynamic range was limited, and that bias levels were critical. First a circuit (appearing in the manufacturer's literature) that configured the LM 1496 as a frequency doubler was built. The same frequency was applied to the L and R ports except that the L port signal was phase shifted 90° by a capacitor. The circuit would function only when the input and bias levels were set at a particular value. Changes on the order of ±0.1 V would distort the I port output signal.

The instrument builders chose to use a unipolar digital signal as the L port input. This signal comes from a 74LS324 digital VCO. This was a design convenience but it should be remembered that the mixer will try to output a true product of the L and R ports and that the L port does have a 100-MHz bandwidth. Figure 8 shows the results of multiplying a square wave with a sine wave using the breadboarded LM 1496. Perhaps the design thinking was that the truncated signals would be smoothed by the filter anyway. Still, output power is lost, and more undesired frequencies are present in the output signal. The unipolar waveform must be carefully biased to cause the desired diode switching.

The I port output signal is buffered by an LH002 current amplifier. Its output begins to roll off at about 10 MHz. It serves to remove spiky edges from the output of the mixer-multiplier, though this is probably an unintentional prefilter. Its principal purpose is to buffer the mixer-multiplier from the filter. Visual observation, however, showed that the presence of the filter significantly changed the signal at the mixer-multiplier output in spite of the presence of LH002 buffer. Another possibly unintentional benefit of the buffer is that there is a lot of L port feedthrough that is suppressed by the current buffer amplifier.

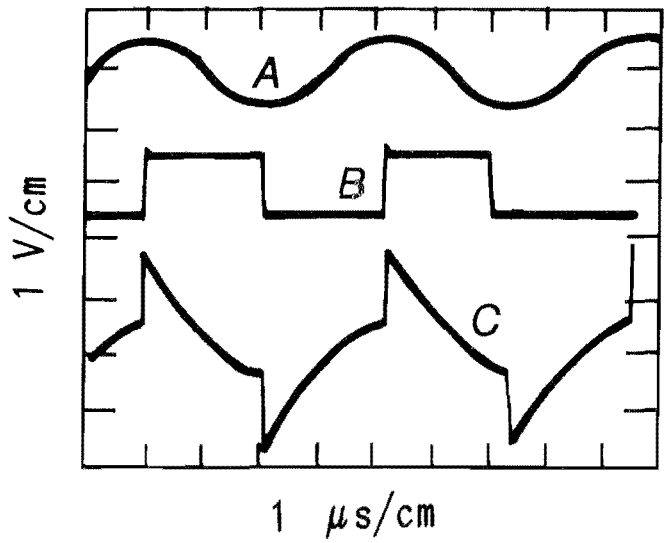

Figure 8.–Multiplying a sine wave (*A*) by a square wave (*B*) to produce a product signal (*C*).

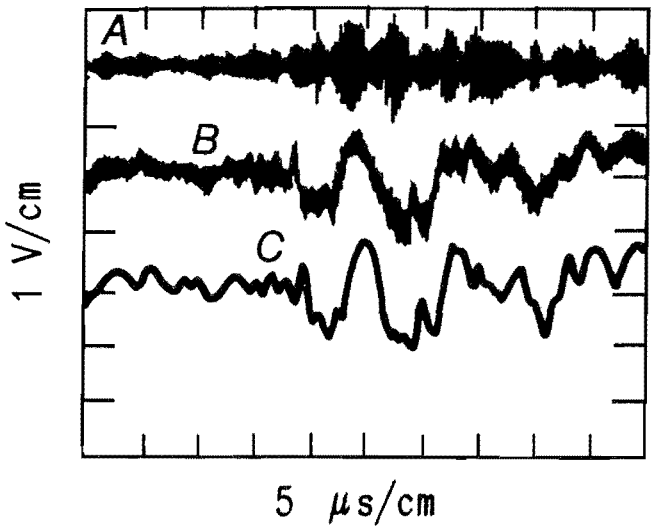

Figure 9–Actual response of LM 1496 modulator-demodulator and custom filter. *A*, Reflection signal; *B*, LM 1496 output; *C*, filter output.

The filter is a custom-built LRC filter containing three handwound inductors. It seemed to be generally functional with a low-pass bandwidth of about 1 MHz. However, its presence significantly altered the output of the mixer-multiplier. It apparently reflects signals back into the I port or otherwise loads the LM 1496.

Figure 9 shows the actual output of the I port with the tested instrument in phase lock on a mine roof bolt. The filter output tends to oscillate near the filter cutoff rather than at the difference frequency as would be expected, and it always contains some high-frequency ripple. Realizing that the probing and reflection frequencies are in fact not equal, the filter output might appear to have some general resemblance to the expected output, but it is far from the simple sinusoidal variation expected. The output represents a nonideal mixer-multiplier output, distortion from the filter loading, prefiltering by the buffer amplifier, and finally processing through an LRC filter.

Because of the dependence of the multiplier output on signal amplitude and because of the presences of higher frequency modulation in the multiplier output, significant deviations from expected performance can occur. Zero crossings of the appropriate slope to cause lock can appear and disappear and can repeat frequently. The deviation from theoretical performance accounts for the remainder of the observed P^2L^2 deviations from ideal performance not already explained by the transducer related problems.

The behavior of the whole system, including the transducer resonance and circuit performance, is so nonideal compared to the original theory that it would be logical to question why it functions at all. Yet from the experiments, it obviously functions to a significant degree and, in special circumstances, shows very stable performance. The VCO does not discern the nature of its controlling input from the mixer-multiplier. It only reacts to the magnitude and sign of the control voltage. As long as the filter output takes on positive and negative values passing through zero with negative slope at some point or points as the L port input frequency changes, the electronic locking criteria can be met. If the filter output is additionally a repeatable waveform for a given reflector distance, then the instrument can function to some degree. The sample and hold, which is needed to hold the VCO steady between tone bursts, also serves to minimize problems that might otherwise be present from the filter output that differs so markedly from the theoretically expected DC level.

Consider also that the errors discussed arise from only the last fraction of a cycle counted. If a 2.25-MHz transducer and 2.25-MHz probing frequency are used, a phase error of ±13° would represent a time error of about 1.6×10^{-8} s. This time, as it relates to actual strain in a steel bolt, is operated on by a factor of 0.28 to represent the length-caused time change separated from the velocity-caused time change. The net effect is that the 13° phase error would represent only about a 100-lbf load error in a 4-ft bolt. Even a relatively inaccurate circuit can then produce relatively precise results in terms of load. With shorter reflector distances, the same 13° error represents a proportionally higher load error, which would soon become unacceptable for the mine roof bolt application. To use a 15-in reflector, which is typical for mine bolt experiments, and measure 50-lbf load change, the overall phase lock-loop errors would have to be held to about ±2°.

CONCLUSIONS

The overall conclusion of the P^2L^2 research is that both general and instrument-specific P^2L^2 problems would have to be solved before this technology could be applied to mine roof bolt load measurement. Because some of this research is applicable to other P^2L^2 technology uses and because P^2L^2 technology offers the promise of significantly higher resolution than pulse-echo technology, it is appropriate to discuss further details in this conclusion. These fall into the general category of transducer problems, mathematical problems, and circuit problems.

The most significant obstacle to creating a truly stable P^2L^2 instrument appears to be to develop or discover a suitable nonresonant transducer. It must transceive a signal that follows the driving frequency exactly. It must be efficient enough to allow for the reception of a usable level of received signal. There is a suggestion in the literature that construction of a nonresonant transducer is possible. A research program would have to be established to determine if a suitable transducer can be developed. The remnant effects on the reflection frequency by bolt resonance harmonics and multiple signal paths would then also have to be studied. Possibly a type of filter that would track the driving frequency could be employed to focus only on the desired frequency.

There is no reason to make the mathematical errors such as using F_i instead of F_f as the normalizing frequency or of dropping significant terms in equations relating strain to frequency or time changes. Proper derivations and equations have been provided by this report These derivations also show that there is a simple physical and mathematical equivalence between time change measurement and properly normalized frequency-change measurement. The frequency change measurement does, however, require repeatedly updated normalization with the current frequency, whereas the time needs only to be normalized by the constant initial travel time. Either measurement can be equivalently related to strain or stress. Though it is widely ignored in the literature, velocity does exhibit small nonlinearities that must be accounted for in high-precision measurements performed with either type of instrument.

There is no obvious electronic reason that the hardware of the P^2L^2 instrument itself could not be made to function in accord with expected results. Proper selection of components should accomplish this goal. A given circuit might be limited to processing reflections within a set amplitude range, but the operator could be alerted to out-of-range signals, or gain adjustments might be automatically made. Using a bipolar simple sinusoidal signal to drive the transducer might help reduce transducer resonance effects. Digital multiplication of the signals might be possible and beneficial in eliminating unwanted analog mixer products and extending dynamic range where digitizing speeds could be made sufficient to handle required system frequencies and repetition rates.

With currently available transducers and instruments, the instability due to apparent resonance frequencies and their variability is always present. Likewise, the instability of the reflection wave shape seems always to be present. Only the driving frequency is controlled and measured. The magnitude of the resulting error can be reduced by setting the driving frequency very near to the mounted resonance of the transducer and holding all other environmental factors and transducer position constant. The significance of the remnant errors will depend on the particular measurement being made. Just having different driving and reflection frequencies present places the operation of the instrument outside the bounds of the theory. For a given type of bolt or other measured object, it is prudent to calculate expected frequency change per load increment and compare it to observed values. Substantial deviations should cast doubt on the conformance of collected data to instrument theory.

Relationship between stress or load and frequency becomes empirical even if the reflection frequency is constant. If the frequencies are close and the gauge length is long, all of the unequal frequency errors might, for a given measurement situation, always range within an acceptable measurement tolerance, such as ±100-lbf load equivalent. If the frequencies are not close or the gauge length is short, these errors may be completely unacceptable. Until a nonresonant transducer is developed, such errors will always be present in the tested instruments. Using the tested instrument to discern subtle changes in material behavior under thermal or other change was not possible for these reasons. Changes related to the drift of F_2 and to its nonequality with F_1 would cast doubt on any speculation that a particular change was related to any real physical phenomena.

Because the value of F_2 is affected by so many factors in complex ways and is variable, it is very difficult to establish a specific degree of confidence in a measurement. Only in special cases where there was thermal isolation, time was allowed for couplant movement to settle, and loads were not changed could truly stable measurements be made. The nonideal behavior of the electronics similarly would cast doubt on the theoretical meaning of high-precision measurements made with the tested instruments.

Trying to make alterations to the P^2L^2 technology to make it work for mine roof bolt load measurement exceeded the scope of the research project when an alternative technology (pulse-echo) was found to be suitable and free of major problems. It is hoped, however, that the research accomplished on the P^2L^2 technology and discussed in this report will serve to make other researchers aware of possible problems, provide solutions to some problems, and stimulate others to develop stable P^2L^2 instruments that fulfill the promise of an order of magnitude increase in resolution.

REFERENCES

1. U.S. Code of Federal Regulations. Title 30–Mineral Resources; Chapter I–Mine Safety and Health Administration, Department of Labor; Subchapter O–Coal Mine Safety and Health; Part 75–Mandatory Safety Standards–Underground Coal Mines; Part C–Roof Support; Sec. 75.204-Roof Bolting; July 1, 1988.

2. Steblay, B. J. New Instrumentation for Roof Bolt Load Measurement. IEEE Trans., v. 1A023, No. 4, July/Aug. 1987, pp. 731-735.

3. Bickford, J. H. An Introduction to the Design and Behavior of Bolted Joints. Marcel Dekker, Inc., 1981 , 443 pp.

4. Heyman, J., and E. T. Chern. Ultrasonic Measurement of Axial Stress. J. Test. and Eval., v. 10, No. 5, Sept. 1982, pp. 202-211.

5. Heyman, J., and W. Issler. Ultrasonic Mapping of Internal Stresses. Paper in IEEE Ultrasonics Symposium Proceedings, Oct. 1982 IEEE, 1982, pp. 92-97.

6. Hughes, D. S., and J. L. Kelly. Second Order Elastic Deformation of Solids. Phys. Rev., v. 92, No. 5, Dec. 1953, pp. 1145-1149.

7. Mao, N., J. Sweeney, J. Hanson, and M. Constantino. Using a Sonic Technique to Estimate In Situ Stresses. Paper in Proceedings of the 25th Symposium on Rock Mechanics, Evanston, IL, June 25-27, 1984. Soc. Min. Eng. AIME, 1984, pp. 167-175.

8. Maleki, H. N., M. P. Hardy, C. J. H. BrestVanKampen. Evaluation of Roof Bolt Tension Measuring Techniques. Paper in Proceedings of 26th U.S. Symposium on Rock Mechanics. A. A. Balkema, v. 1, 1985, pp. 425-437.

9. Hegsen, R.C. Broadband Ultrasonic Transducers. NASA Tech. Briefs, v. 10, No. 2, Mar. 1986, p. 47.

10. Henderson, B. C. Mixers Characteristics and Performance, Theory and Technology. Watkins-Johnson Co. Tech. Notes, v. 8, No. 2, Apr.-June 1981, 15 pp.

11. _____. Mixers Characteristics and Performance, Theory and Technology. Watkins-Johnson Co. Tech. Notes, v. 8, No. 3, Apr.-June 1981, 19 pp.

APPENDIX.–SYMBOLS USED IN THIS REPORT

DC	0 frequency
e	error in quadrature lock
E_0	output voltage from multiplier circuit
f	lock frequency
F	frequency
F_i	no-load (initial) frequency
F_t	current (present) frequency
G	VCO voltage-to-frequency conversion factor
M	amplitude
N	integer number of cycles between the start of a tone burst and the position of the sample point
ℓ	path length
t	time
T	stress
V	velocity
VCO	voltage-controlled oscillator
γ	angle quantity
Δ	delta meaning incremental difference (Δt is the difference in t)
θ	phase difference angle between the reflection and the continuation of the driving tone burst as measured at the beginning of the reflection tone burst.
π	radian
ρ	density
ϕ	net phase difference angle between driving and received signals
ω	angular velocity
ωt	is simply an equation team formed by multiplying ω and t which have already been defined.